American Journal of Polymer Science and Technology
2026, Vol. 12, No. 1, pp. 17–37
https://doi.org/10.11648/j.ajpst.20261201.12

SciencePG
Science Publishing Group

Review Article

A Review of Recent Advances and Techniques Used in the Fabrication of Coatings on Micro/nanostructured Anti-wetting Surfaces

Diawo Diallo*, Djibril Diouf, Abdoulaye Drame, Alioune Diouf

Department of Chemistry, University Cheikh Anta Diop, Dakar, Senegal

Abstract

Anti-wetting surfaces, which possess strong water-repellent properties and self-cleaning, anti-fouling, anti-icing, and anti-corrosion characteristics, are of great interest due to their numerous applications across various industrial sectors. For thousands of years, nature has developed highly innovative wetting systems to survive in hostile environments. For example, the surface structures of lotus leaves and gecko feet, with their superhydrophobic and parahydrophobic properties, play a key role in the adhesion of these natural surfaces. This review article examines in detail the theoretical foundations, various fabrication techniques, applications, and challenges associated with anti-wetting surfaces. This literature review analyzes the fundamental principles, focusing on water-repellent surfaces observed in nature, theories of wettability such as Young's equation, the Wenzel and Cassie-Baxter states, as well as the dynamics of wetting. Various techniques for fabricating anti-wetting surfaces, such as dip-coating, templates, the sol-gel technique, etching, and electropolymerization, are studied, ranging from micro- and/or nanostructuring methods to advanced material coatings, highlighting the evolution of surface engineering. The numerous applications of water-repellent surfaces, ranging from self-cleaning technologies to oil-water separation, are discussed, highlighting their potential contributions in fields such as energy, environmental protection, and anti-icing. Despite their promising properties, water-repellent surfaces also face significant challenges, such as issues of durability and scalability, environmental concerns, and limitations in achieving multifunctionality. By providing a comprehensive overview of the current state of research on anti-wetting surfaces, this review aims to guide future studies and encourage innovations in the development and use of these intriguing surfaces.

Keywords

Anti-wetting Surfaces, Fabrication Techniques, Coatings, Wettability Theories, Applications

1. Introduction

Controlling the wettability of surfaces for the development of innovative materials in various fields is now more important than ever, given the wide range of applications that result from it. Research conducted on animal and plant species [1, 2], has revealed that surface wettability depends primarily on the relationships between physicochemical properties. Today, through a biomimetic approach inspired by nature, several processes have been developed to replicate these micro- and/or nanostructured surfaces, with the aim of achieving spe-

*Correspondence: Diawo Diallo (diawo.diallo@ucad.edu.sn)

Received: 22 May 2026; **Accepted:** 10 June 2026; **Published:** 29 June 2026

cific wettability properties. The combination of an intrinsically hydrophobic chemical composition and multi-scale texturing is believed to be responsible for the rather unique surface properties of these materials, such as the lotus effect or the gecko effect [3, 4]. It is in this context that mathematical equations such as those of Wenzel and Cassie-Baxter [5, 6] were established to explain the possibility of increasing or reducing hydrophobicity by manipulating surface texturing. Mastering the optimal conditions regarding material composition therefore begins with selecting the molecular structure or core that offers the best performance. Superhydrophobic and parahydrophobic materials are important for applications like self-cleaning windows, anti-wear, antibacterial uses, and waterproof textiles [7-21]. Various methods for creating micro- and nanostructured surfaces include chemical and physical treatments like lithography and etching [22]. Conductive polymers can develop these materials with unique surface textures through self-assembly and direct application [23]. This manuscript reviews these surfaces, starting with a biomimetic approach that looks at natural surfaces with special properties. It will explain wetting phenomena and detail the Wenzel and Cassie-Baxter models, followed by methods for making water-repellent surfaces and their potential applications.

2. Natural Hydrophobic Surfaces

Observation of the surface properties of certain plant species has revealed extreme wetting phenomena, such as the self-cleaning ability of certain leaves in rainy weather when a water droplet comes into contact with their surfaces, and, conversely, strong adhesion phenomena over a small solid-liquid contact area [24]. Interesting wetting phenomena have also been observed in animals, such as the ability of certain insects to glide on water or the ease with which certain species of sharks move while hunting their prey [25, 26]. It is through these natural wetting phenomena that the scientific community drew inspiration to ultimately reproduce them artificially using the same strategy [27]. In this section, we will present the various wetting phenomena in plant and animal species to provide an overview of the majority of wetting phenomena described in the literature.

2.1. Non-wetting Surfaces in Plant Species

The leaf of Nelumbo nucifera, or lotus, exemplifies extreme wetting with its self-cleaning property known as the Lotus effect [2, 27, 28]. Water droplets bead and roll off the leaf at low angles, effectively removing dirt. This phenomenon arises from the leaf's unique surface structure, which includes micropits at the micrometer scale and hydrophobic wax crystals at the nanometer scale, contributing to superhydrophobicity by limiting liquid penetration and repelling droplets (Figure 1). This phenomenon was demonstrated by Barthlott and Neinhuis [28] by placing a drop of mercury on a superhydrophobic sheet (see Figure 1).

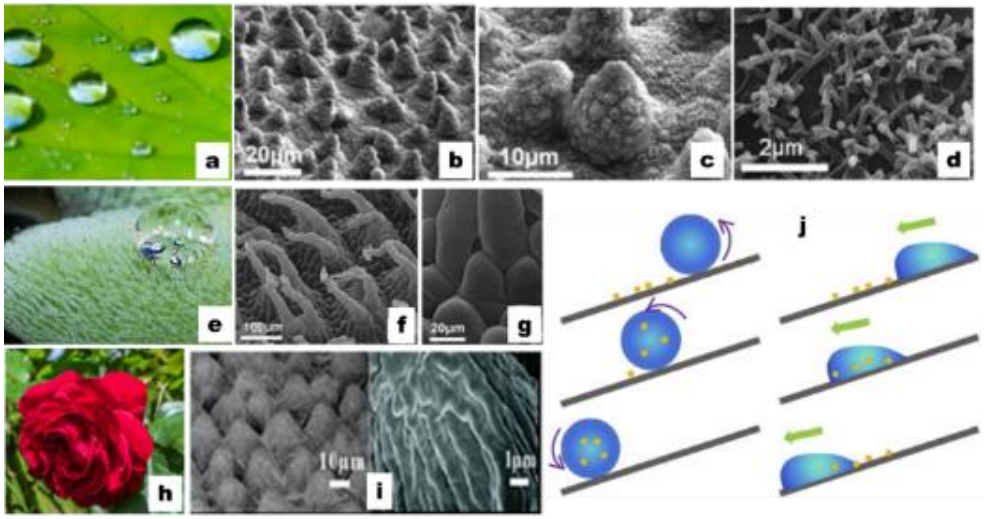

Figure 1. *Photographs and SEM images of the Lotus (a, b, c and d) [2]; SEM image of the leaf hairs of the water fern of the genus Salvinia (e, f and g) [1]; Photograph of a rose petal (h), SEM image (i) [29]; Image illustrating the self-cleaning effect of a droplet on a contaminated surface (j) [28].*

Other plant species, like the genus Salvinia [1], exhibit wettability properties similar to lotus leaves, displaying hydrophobic behavior due to unique micropilie shapes. These multicellular hairs, visible to the naked eye, form complex surface structures that retain air layers even when submerged. Scanning electron microscopy (SEM) reveals that these hairs comprise small wax rods on the epidermal cells (see Figure 1).

Koch et al. [1] investigated how various plant types' functional surface structures are influenced by their environments. They found that plants in hot environments develop 3D wax crystals or "hairy" surfaces suited for temperature and UV radiation, while those in humid or temperate climates possess smoother or double-structured surfaces affecting liquid spreading behavior (see Figure 2).

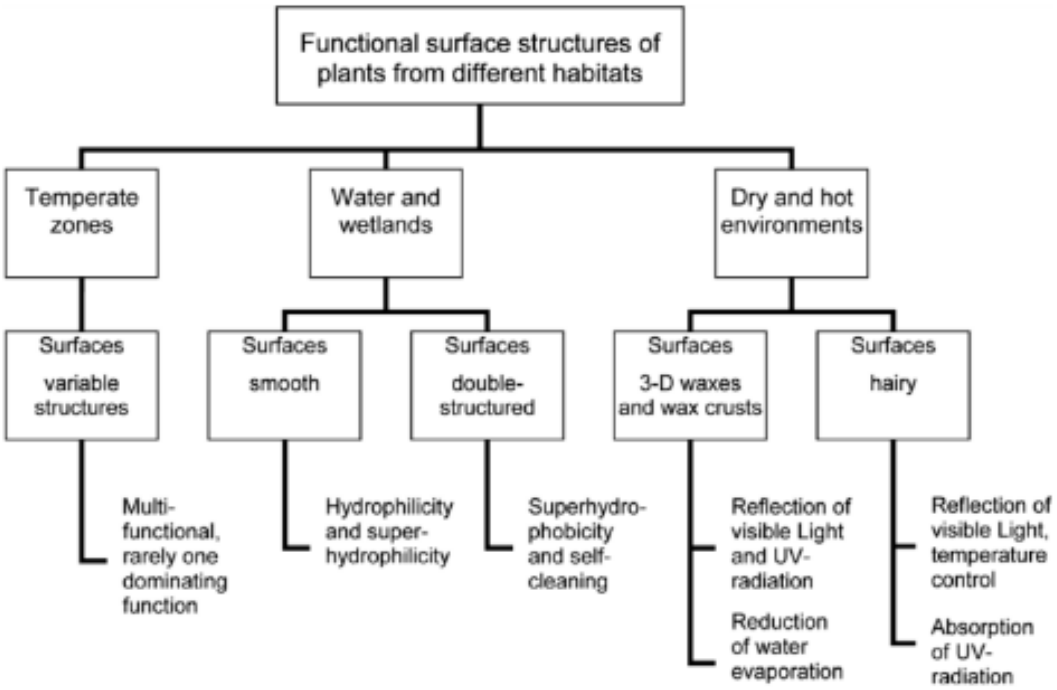

Figure 2. *A tree of characteristic surface structures and functions of plants in temperate environments, aquatic and wetland habitats, and deserts [1].*

We highlight the importance of demonstrating a natural surface with high hydrophobicity and strong water droplet adhesion, termed parahydrophobicity. A prominent example is the rose petal [29], which, as observed through SEM, is covered with micropapillae and nanofolds. These structures create sufficient roughness for superhydrophobicity while maintaining a strong adhesive force with water, causing droplets to remain spherical and unable to roll off the surface, even when inverted (see Figure 1). This effect is known as the Petal Effect.

2.2. Non-wetting Surfaces in Animal Species

Many animal species exhibit extreme water repellency, known as superhydrophobicity, particularly insects, which have been extensively studied. Research by Wagner and al. [30] has explored the correlation between wing microstructures, their wettability, and behavioral responses to contamination in 97 insect species.

Insects demonstrate multifunctional properties such as optical effects and anti-wetting behaviors. Research by Oh et al. [31] on various cicada species, including Neotibicen pruinosus, Neotibicen tibicen, and Megatibicen dorsatus, revealed a relationship between wettability, topology, and droplet-jumping on wings, influenced by habitat and life cycle (see Figure 3). The study found these species possess superhydrophobic wings with truncated conical pillar morphology at the nanoscale, leading to stable water droplet bouncing behavior.

Other insects display diverse surface properties, including light diffraction and water resistance. Research led by Zheng et al. [32] on butterflies like Morpho Aega highlights the hydrophobic and anisotropic traits of their wings, where specific surface structures direct water away, causing droplets to roll off. This orientation affects droplet movement, resulting in them adhering to the wings instead. Additionally, terrestrial animals have been examined for their surface textures. For example, Geckos [4], desert-dwelling reptiles with hydrophobic skin (see Figure 3), can climb vertical walls and ceilings due to their legs covered with micro- and nano-hairs known as setae. These structures enhance adhesion on solid-liquid surfaces, generating Van der Waals forces that enable them to defy gravity in various positions. Studies on water-repellent surfaces, particularly shark skin [33, 34], reveal that its dermal denticles feature specially sized riblets aligned with swimming direction (see Figure 3). This microstructure efficiently manages natural vortices, decreasing energy transfer and shear stress, which reduces drag and enhances underwater movement [26].

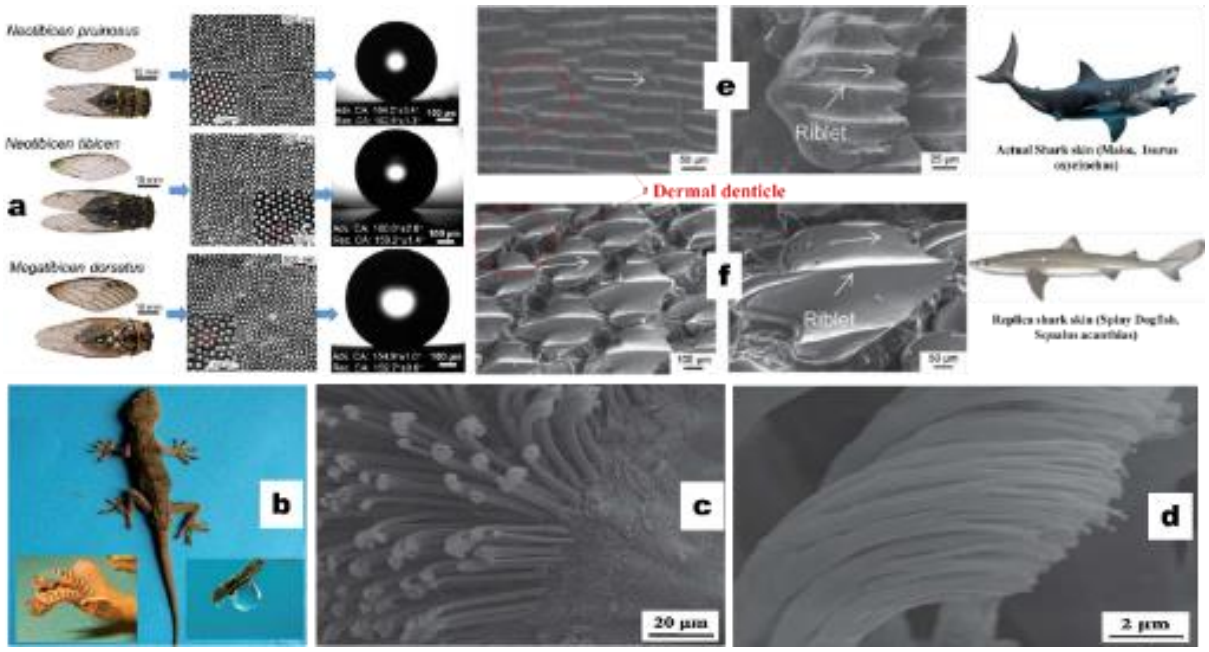

Figure 3. *Topography, SEM images, and water wettability of the wings of Neotibicen pruinosus, Neotibicen tibicen, and Megatibicen dorsatus(a) [31]; Photographie d'un gecko ainsi que sa patte (b) et son image MEB à different grossissement (c, d) [4]; Photographs and SEM images of shark skin samples taken from live specimens. Mako (e) and a specimen of a spiny dogfish (f) [34].*

3. Theories of the Wettability of Water-repellent Surfaces

Wettability refers to the interaction between a liquid droplet and a solid surface, crucial in industries such as chemicals, automotive, and life sciences. In automotive applications, it influences surface preparation for paint and tire traction. In life sciences, surfactants assist lung expansion at birth by reducing surface energy. The behavior of a droplet on a solid can result in either spreading or a hemispherical shape, influencing the contact angle: angles under 10 °denote superhydrophilic surfaces, while those over 150 °indicate superhydrophobic surfaces (see Figure 4) [27, 35, 36].

In order to characterize the adhesive properties of a droplet on a surface, it is necessary to measure dynamic contact angles such as the angles during approach and retreat, and thus the hysteresis while the surface is tilted.

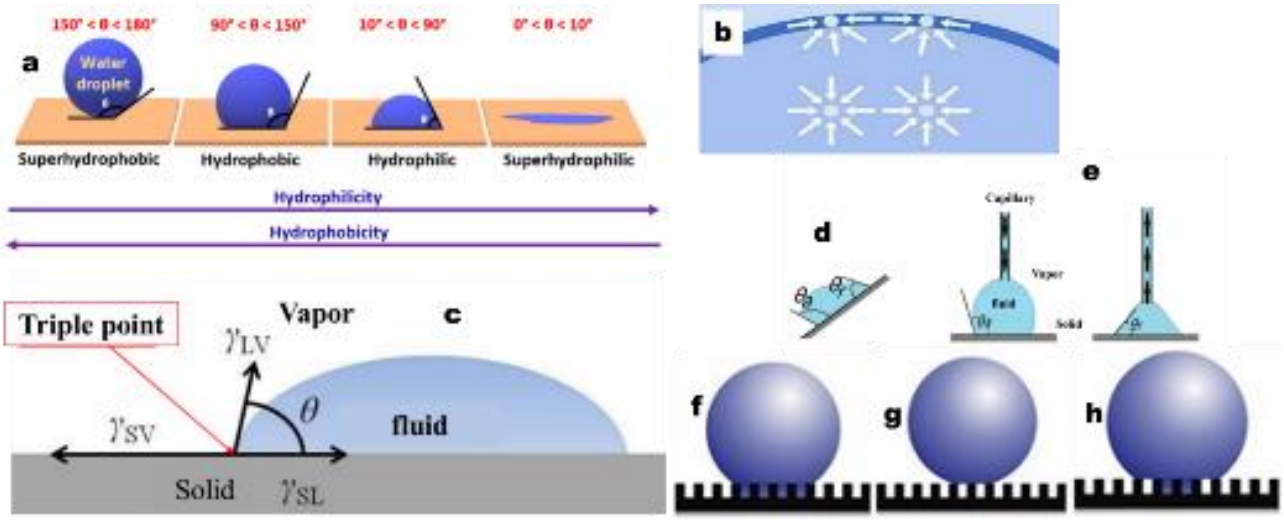

Figure 4. *Diagram illustrating various surface wettability's through contact angle measurements (a) [27]; Surface tension at a liquid-solid interface caused by molecular imbalance (b) [37]; Static contact angle of a liquid droplet at equilibrium on a solid substrate (c); Forward and backward angles of a drop's movement on an inclined surface (d) and during the expansion and contraction of a drop (e) [38]; Diagram of models of a liquid droplet on a rough surface: (f) Wenzel model; (g) Cassie-Baxter model; (h) Wenzel-Cassie transition state [39].*

3.1. Concept of Surface Tension and Surface Energy

Surface energy (γ) is the energy required to increase the interface area between two phases without changing their volume. Molecules at the surface differ from those in the bulk due to contact with fewer neighbors, resulting in higher potential energy (Figure 4). Solids minimize surface area to reduce this energy, and liquid droplets adopt a spherical shape to minimize the surface-to-volume ratio. Surface energy and tension share dimensions, typically represented as force per length (N/m) or work per unit area (J/m). The surface energy of a liquid equals its surface tension, but the measurement of solid surface energy requires calculating from liquid/solid contact angles. Factors like temperature can influence surface tension. For measuring nonpolar surfaces, nonpolar test liquids are used without focusing on specific molecular interactions; for polar surfaces, polar liquids are required, emphasizing molecular interactions relating to functional groups like hydroxyl and carbonyl [37]. The surface energies were calculated using the Owens-Wendt equation [40] with water, diiodomethane, and hexadecane as the three liquids. These calculations applied solely to smooth surfaces, as surface roughness influences contact angles but not surface energy.

3.2. Smooth Surfaces

3.2.1. Young's Theory

Young's theory serves as the starting point for wetting models, which are based on the equilibrium of interaction forces along the triple line. It determines the static contact angle of a sessile droplet on an ideal, "smooth," homogeneous, rigid, and insoluble solid surface (Figure 4). As shown in Equation 1, according to Young's equation [41], the static contact angle depends solely on the thermodynamic equilibrium of the surface tension at the solid (S)-liquid (L)-vapor (V) interfaces [42]:

$$\cos\theta_y = \frac{\gamma_{SV}-\gamma_{SL}}{\gamma_{LV}} \quad (1)$$

Where: θ_y = Young's contact angle,
γ_{SV} = surface tension at solid-vapor interfaces,
γ_{SL} = surface tension at solid-liquid interfaces,
γ_{LV} = surface tension at liquid-vapor interfaces.

3.2.2. Hysteresis of the Contact Angle

Young's equation suggests a single contact angle for a solid, liquid, and vapor, but in reality, a range of contact angles appears due to factors like the receding and advancing angles. Superhydrophobic surfaces are not just defined by angles over 150 ° [27, 43]. The surfaces show various irregularities, leading to contact angle hysteresis, which is the result of imperfections allowing the contact line to stick. When a droplet is on an inclined surface, it resists movement until it reaches a slip angle, after which it rolls. The advancing angle, θa, and retreating angle, θr, define this behavior Equation (2), with the difference indicating contact angle hysteresis, H (Figure 4).

$$H = \theta_a - \theta_r \quad (2)$$

To visualize contact angle hysteresis, place a liquid droplet on a smooth surface and enlarge it using a capillary tube [38] (Figure 4). The contact angle increases until a critical angle is reached, causing the triple point to shift (advance angle θa). Reducing the droplet's volume decreases the contact angle until the triple point moves closer (retraction contact angle θr). It is generally accepted that a parahydrophobic surface must have a contact angle hysteresis greater than 10 °and a contact angle exceeding 90 °[27, 44]. Conversely, with a hysteresis of less than 10 °, the surface is classified as superhydrophobic, indicating that the parahydrophobic state is an intermediate condition [36]. Many natural surfaces are not perfectly smooth and thus exhibit roughness, which complicates Young's equation's ability to predict contact angles. To evaluate surface wettability accurately, the effects of surface roughness must be considered. Two models, the Wenzel model and the Cassie-Baxter model, have been proposed to describe wetting states on rough surfaces [27, 44], both relying on Young's angle θy.

3.3. Rough Surfaces

The roughness of a solid describes its surface shape at a small scale. It is defined by comparing the actual surface area, including peaks and valleys, to the smooth geometric area. This helps calculate the roughness factor, r:

$$r = \frac{\text{Surface reel}}{\text{Surface planaire}} \quad (3)$$

The influence of surface roughness has been described by Wenzel and Cassie–Baxter [27].

In 1936, Wenzel studied how surface roughness affects wetting behavior, leading to Wenzel's equation:

$$\cos\theta_W = r \times \cos\theta_y \quad (4)$$

The Wenzel angle (θw) relates to the surface roughness factor (r), which compares actual surface area to projected area. Wenzel's equation shows that increased roughness enhances wettability. A smooth hydrophilic surface becomes more hydrophilic, while a hydrophobic surface becomes more hydrophobic with increased roughness. (Figure 4).

The model by Cassie-Baxter from 1944 suggests that on rough surfaces, air pockets form between water and the surface, reducing contact area. This results in a heterogeneous wetting regime described by the Cassie-Baxter equation:

$$\cos\theta_{CB} = \phi_S\left(r_\phi \times \cos\theta_y + 1\right) - 1 \quad (5)$$

The Cassie-Baxter contact angle (θ_{CB}), solid-liquid contact area fraction (ϕ_s), and Young contact angle (θ_y) relate to surface roughness. Increased roughness traps more air, decreasing ϕ_s and increasing the contact angle. This affects droplet dynamics on rough surfaces, enhancing hydrophobicity and hydrophilicity [27].

The Wenzel model has high static and advancing contact angles but low receding angles, leading to high hysteresis and adhesion. The Cassie-Baxter model features mobile droplets with high contact angles and low hysteresis, crucial for superhydrophobicity [45]. A transition between wetting types occurs when a droplet's volume increases due to external forces, changing its interaction with the surface (Figure 4). For self-cleaning, the Cassie-Baxter state is ideal for dust, while the Wenzel state captures water. Surface treatments can adjust wettability and roughness [46].

4. Approach to the Development of Structured Water-repellent Surfaces (Hierarchical)

Superhydrophobic surfaces can be made using various materials, both organic and inorganic. For polymers, the goal is to create surface roughness, while inorganic materials require hydrophobic treatments after shaping. Techniques for making these surfaces fall into two categories [27, 44, 47–50]: creating rough surfaces from low-energy materials and modifying rough surfaces with low-energy materials. Various methods are used to prepare rough surfaces, such as dip-coating, templates, the sol-gel technique, etching, and electropolymerization, better known as electrochemical polymerization [22]. A brief description and the applications of some of these important techniques are presented in the following subsections.

4.1. Chemical and Physical Etching

Lotus leaves exemplify superhydrophobic surfaces, featuring a dual-layer structure at micro and nanoscale levels, completely coated with natural hydrophobic waxes (Figure 5). Their contact angle exceeds 160 °, keeping the surface clean even when soiled. An etching technique emulates these natural structures to improve surface roughness, thereby enhancing superhydrophobicity [51]. The etching technique is inspired by natural structures to enhance surface roughness, creating superhydrophobic surfaces. Differences in etching rates among crystal planes lead to increased roughness, and a low surface energy material is then applied to achieve superhydrophobicity [37]. Etching has two main types: dry etching, like plasma and reactive ion etching, which uses gases to etch surfaces, and wet chemical etching, which uses acidic or basic solutions on metals. Wet etching destroys dislocation sites, causing surface roughness [52]. In previous studies, superhydrophobic cotton was produced using the wet-coating etching technique [37]. Cotton is treated with sodium hydroxide to develop a rough surface and then coated with silica nanoparticles using heat and acid catalysts, achieving superhydrophobic properties with a contact angle of 176 °. Although chemical etching is cost-effective and scalable, it uses hazardous acids, raising environmental concerns (Figure 5).

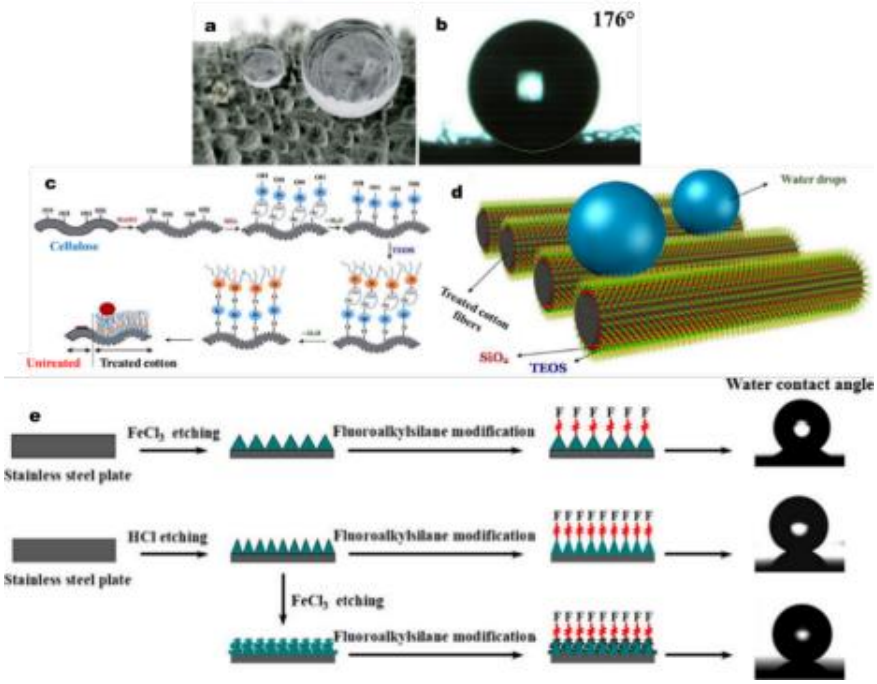

Figure 5. *(a) Double lotus-leaf structures; (b) water droplets on superhydrophobic cotton; (c) chemical etching of cotton fibers; (d) schematic illustration of treated cotton fibers [37]; Superhydrophobic surface on stainless steel produced by a two-step chemical etching process [53].*

The outermost layers can be removed by physical etching. The primary technique is plasma ablation [37]. This technique is simpler, cheaper, and less harmful to the environment. It uses electrons to bombard samples at low pressure, often in oxygen. It allows for selective surface treatment with lasers, where treatment time and laser intensity control the degree of modification, particularly for cotton fabric. [54]. Materials inspired by water-walking insects have been developed by Wang and al. [55]. Zhang and al. [53] developed superhydrophobic surfaces on stainless steel substrates using a two-step chemical etching method. The substrates are immersed in solutions of hydrochloric acid and ferric chloride to form microstructures. The resulting surfaces have a contact angle of 159 ° and a sliding angle of 2 °(see Figure 5). The superhydrophobic surfaces produced in this way demonstrated excellent stability and self-cleaning properties. Recently, other researchers have used chemical etching and a self-assembled monolayer (SAM) coating to fabricate superhydrophobic surfaces on SUS 316 stainless steel [56]. The etching process created structured surfaces, with a fluorine coating lowering surface energy. A 30-minute sample showed a contact angle of 152 ° and a sliding angle of 2 °.

4.2. Template

Template-based methods utilize predefined membranes to fabricate superhydrophobic surfaces by mimicking natural structures, such as leaves and insect wings [57, 58]. Techniques like etching can achieve the necessary micro- and nanoscale roughness on metal templates [59]. The membranes are either lifted or dissolved for replication, making this method cost-effective, rapid, and reproducible, with the key benefit being the ability to replicate natural surfaces. For example, Peng and al [60]. prepared a PDMS master mold by pouring liquid PDMS directly onto a fresh, natural leaf of Xanthosoma sagittifolium and curing it at 50 ℃ for 4 hours, then removing the cured PDMS mold (Figure 6). Subsequently, this master template was used to prepare a polyaniline replica on cold-rolled steel. The superhydrophobic polyaniline film exhibited a micro and nanoscale surface morphology nearly identical to that of the natural leaf.

Dai and al. [63] replicated rose petal surfaces using flexible PDMS substrates for nanostructure growth (see Figure 6). They cured a PDMS prepolymer on the petal, created a positive replica, which revealed a superhydrophobic surface with a contact angle of 153 °. Researchers have mimicked superhydrophobic biological surfaces using polymers. Zhang and al. [62] developed strong membranes using a PVDF solution on stainless steel, creating the M-300F (see Figure 6), which has excellent flow rates and water rejection. Recently, air microbubbles are used to create a system that mimics octopus suction cups [61] (see Figure 6). This system shows strong and reversible adhesion to various surfaces and can transport silicon wafers without contamination.

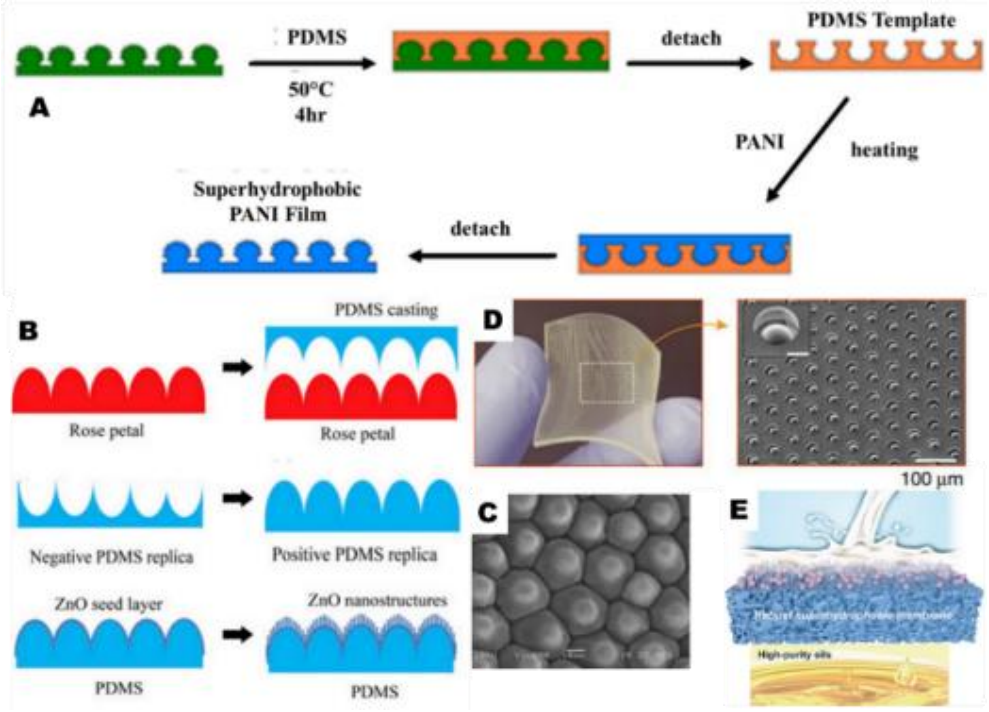

Figure 6. *Schematic of the Templat process for fabricating hierarchical structures: (A) Preparation of a superhydrophobic polyaniline (PANI) film using the template replication method [60] (B) Preparing superhydrophobic ZnO on PDMS from rose petal; (C) SEM image and measurement of the water contact angle of the positive PDMS replica; (D) Photograph and SEM image of microcavities exhibiting dome-shaped structures resembling protrusions [61]; (E) Robust polyvinylidene fluoride (PVDF)-based membrane on a stainless steel plate [62].*

4.3. The Sol-gel Technique

The sol-gel technique allows for the creation of superhydrophobic surfaces on various materials like textiles, metals, and glass. While it complements other coating methods, it has drawbacks such as feasibility and thickness limits, with heat treatment possibly damaging substrates [37, 50]. The process involves converting precursors into glassy materials through hydrolysis and polycondensation. Surface roughness can be adjusted by changing conditions. For example, coatings using alumina nanoparticles result in rough, self-cleaning surfaces, while those made with silica nanoparticles show increased superhydrophobic properties with more nanoparticles added. Additionally, superhydrophobic coatings can be made using electrospray deposition, maintaining effectiveness even after multiple washes and abrasion cycles (Figure 7) [37].

Researchers created a superhydrophobic methylated silica with a core-shell structure [65]. They prepared silica gel using TEOS, ethanol, and NH_4OH, then added MTMS for methyl groups. The surface achieved a contact angle of 161 °, with over 96% separation efficiency. Recently, Barthwal and al. [27] eported the creation of superhydrophobic graphene aerogel beads using an in situ sol-gel method with octadecylamine [64] (ODA (see Figure 7). These lightweight, porous beads have a water contact angle of 153 ° and show great potential for oil spill treatment.

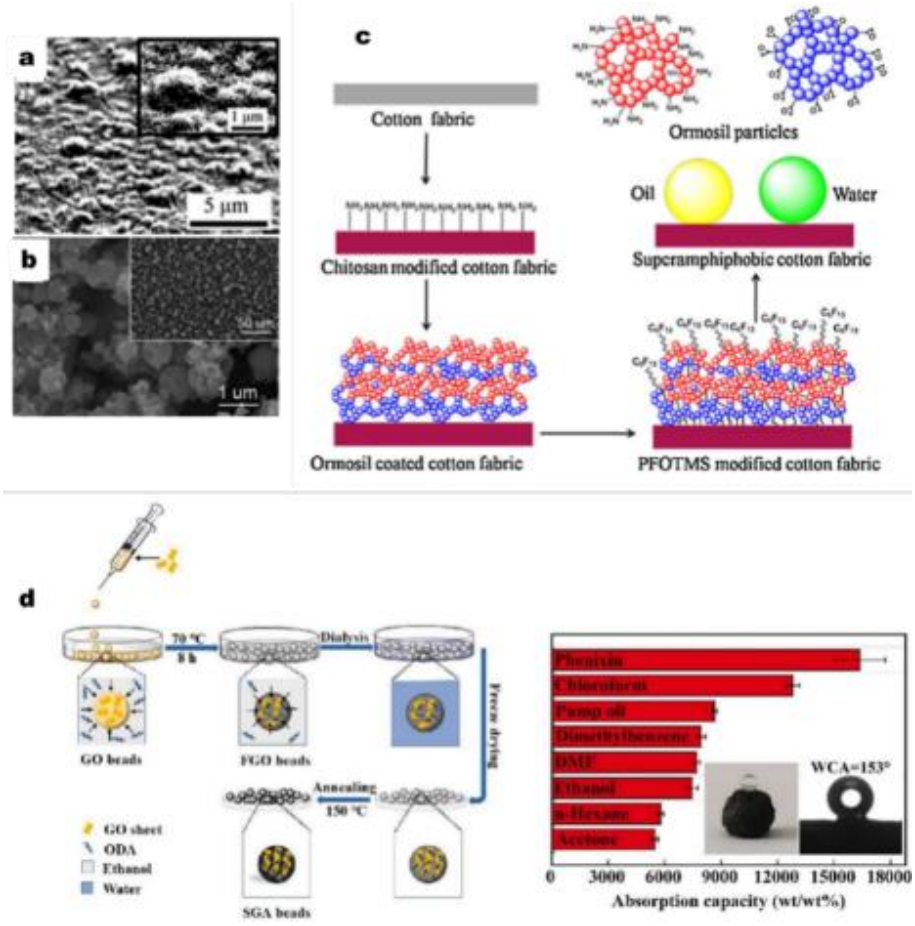

Figure 7. *(a) SEM images of films doped with alumina and nanoparticles after immersion in boiling water, (b) Surface microstructure, observed by FE-SEM, taken from the rough, fluorinated SiO_2 layer prepared at a deposition rate of 0.05 μm/h, (c) Schematic of the manufacturing process for superamphiphobic cotton fabrics [37]; (d) Superhydrophobic graphene aerogel beads for the adsorption of hydrocarbons and organic solvents [64].*

4.4. The Dip-coating Method

The dip-coating technique involves applying a liquid coating solution to a surface. Target materials are dissolved, deposited on the substrate, and then dried to form a film [66–68]. The approach involves dipping a substrate into a coating solution, ensuring complete infiltration before removal. This simple method has complex parameters affecting film thickness and structure, including immersion time, withdrawal speed, and solution conditions. Dip-coating is vital for fluid mechanics and interface science, improving the surface properties of

materials [69]. Sol-gel-based dip coating is a primary modification of solution dip coating, and the deposited films can be better controlled by regulating the preparation of the sol and the subsequent gelation process [70, 71]. Yeom and al. [72] demonstrated that a superhydrophobic sponge can be made using silica nanoparticles and hexadecyltrimethoxysilane, achieving a contact angle over 150 ° and high oil separation efficiency (see Figure 8).

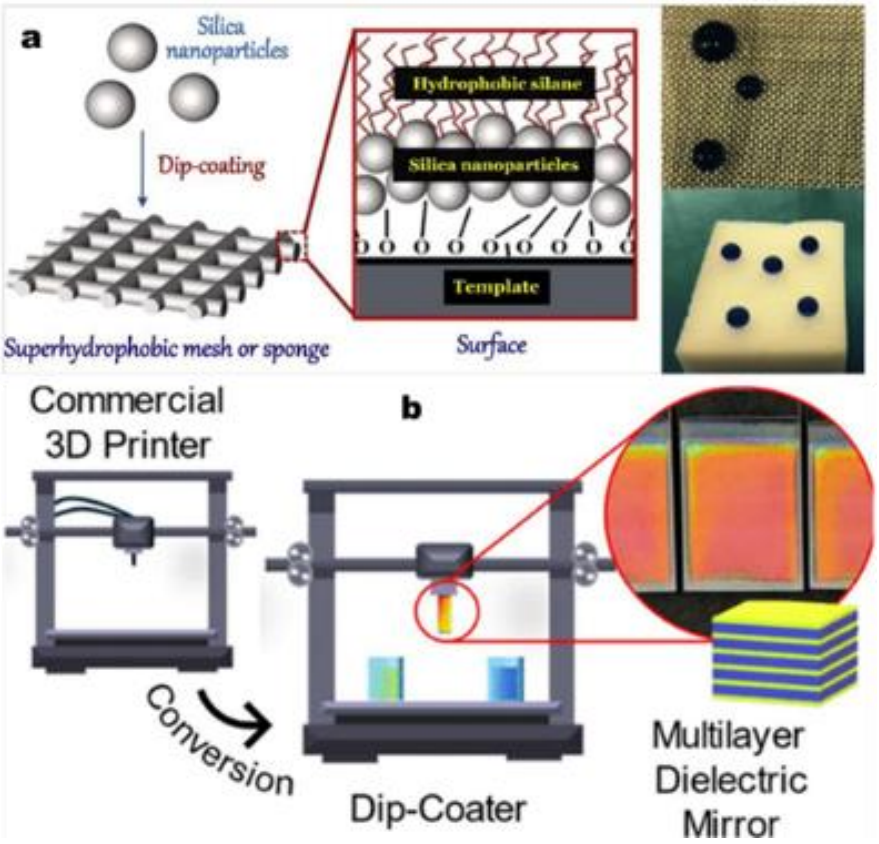

Figure 8. *(a) Superhydrophobic coatings based on nano silica and HDTMS, mesh and sponge treated for the separation of oil/water mixtures [37]; (b) Fabrication of fully polymer multilayer photonic crystals thru the conversion of a 3D printer [73].*

Furthermore, Rauh and al. [74] demonstrated an affordable alternative to these devices by using a 3D printer. This system can automate the coating process by performing multilayer procedures with up to six solutions for six samples, saving time. The thin films of polymethyl methacrylate (PMMA) obtained have a quality comparable to those from a commercial system, and the 3D system can even be better in some cases, making it an interesting option. Recently, other researchers [73] transformed a 3D printer into a coating system to manufacture multilayer photonic crystals using a perfluorinated polymer formulation and poly (N-vinylcarbazole) as structural dielectric media, as well as a recycled mixture of fluorescent polystyrene as a light emitter for the microcavity (Figure 8). They demonstrated that this method works by creating Bragg reflectors and a planar fluorescence microcavity, using specific polymers and controlling the deposition parameters to achieve uniform nanostructures.

4.5. Electrochemical Polymerization (Electropolymerization)

Electropolymerization, or electrochemical polymerization, is a process used since the 1960s [75] to create polymer films. It involves depositing a polymer onto a working electrode from a solution of monomer, solvent, and a supporting electrolyte. This process enhances conductivity and maintains charge balance in the polymer through electron transfer between the electrode and the monomer. Polymerization occurs by oxidizing monomers using an electric current in a solution of electrolyte and dissolved monomer [75]. This process takes place in an electrochemical cell with two electrodes (Figure 9) (below)): a working electrode for polymer film deposition, a reference electrode to measure potential differences, and a counter electrode to complete the circuit.

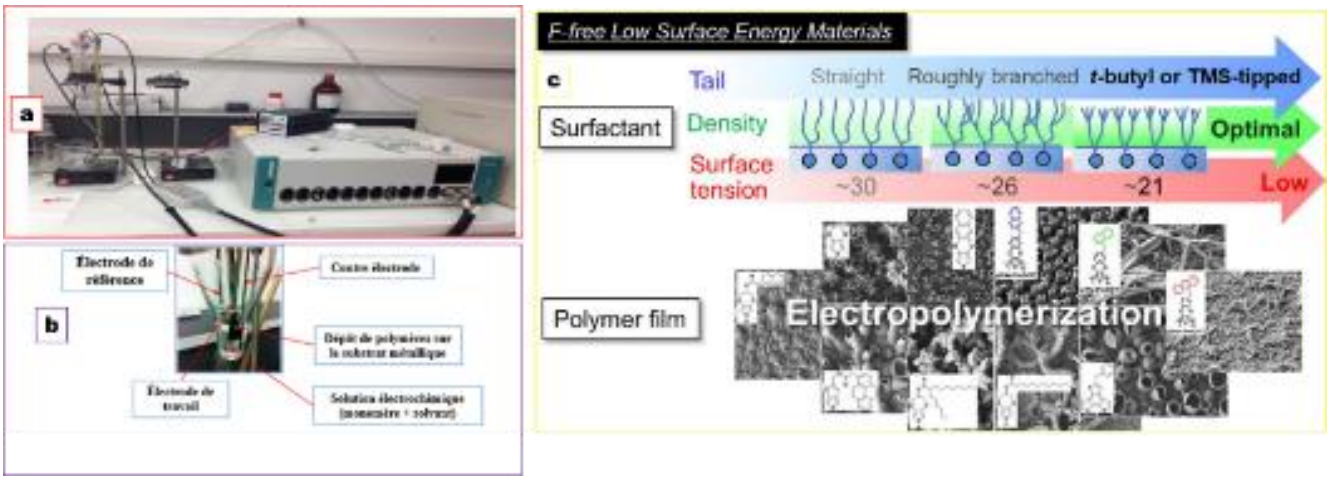

Figure 9. *(a) Photograph of the electrodeposition device and (b) of an electrochemical cell; (c) Surfactants and low surface energy surfaces without fluorine [76].*

Many methods exist for the electrodeposition and doping of pyrrole-based polymers, but the exact mechanism is still unclear. The accepted idea involves oxidizing the monomer at the electrode to create a reactive radical cation, which dimerizes and continues to oxidize, eventually forming a polymer film on the electrode [77]. Electrochemical polymerization is favored for making conductive polymers due to its simplicity and real-time film study capability. Various factors, such as the monomer type and electrochemical method, influence the properties of the polymer films [78-82]. Additionally, methods to create specific coatings, like superhydrophobic surfaces using nickel and PTFE, are discussed [22, 83]. Porous structures can be developed using soft templates and gas bubbles in electrochemical solutions, but there are issues with monomer solubility and bubble stabilization.

Studies by Darmanin and al. [84-93] show that certain aromatic monomers can stabilize gas bubbles. Low-polarity solvents like dichloromethane can dissolve these monomers. In dichloromethane/water systems, micelles form and create porous structures. Thus, new surfactants and low surface energy surfaces without fluorine have been designed thru electropolymerization (see Figure 9) [76].

4.6. Other Methods for the Fabrication of Structured (Hierarchical) Anti-wetting Surfaces

Among the other techniques used to prepare superhydrophobic coatings, one can mention electrodeposition, spraying, chemical vapor deposition, spin-coating, photochemistry, lithography, and electrospinning [22, 50, 94–96]. The choice of an appropriate preparation method depends on the final application. Each method has its own advantages and disadvantages. For example, the spraying method is suitable for treated surfaces and outdoor applications. However, the contact angle is barely 160 °; this method is therefore used for textile applications, construction, and glass. On the other hand, superhydrophobic coatings prepared by spin-coating exhibit low roughness with precise thickness. However, this method is suitable for small surfaces. Lithography is demanding; it is a complicated procedure that makes it difficult to implement on an industrial scale.

5. Applications of Micro and Nano-structured Anti-wetting Surfaces

Materials with anti-wetting properties are increasingly valuable for practical applications, particularly due to hierarchical anti-wetting surfaces. These surfaces exhibit unique hydrophobic and self-cleaning characteristics, making them suitable for self-cleaning windows, tiles, textiles, solar panels, and fluid drag reduction in micro/nano channels [97]. Additionally, their applications extend to agriculture, biomedical fields, stain-resistant textiles, and snow anti-adhesion in antennas and windows [98]. The subsequent section discusses the use of anti-fouling coatings to enhance performance through surface modification.

5.1. Self-cleaning Surfaces

The rising interest in superhydrophobic materials, which feature high contact angles and low water adhesion, is driven by their self-cleaning properties exemplified by the lotus effect. These materials hold promise for applications like self-cleaning windows and paints. Given the ease of contamination in natural environments, developing self-cleaning materials with minimal contaminant adhesion has become a significant research focus over the past few decades.

For example, Nimittrakoolchai and al. [99] developed a superhydrophobic film with anti-adhesion and self-cleaning properties by applying powder and dust. The process involved depositing a polyelectrolyte film on glass, etching it in HCl to

create a rough surface, and adding SiO_2 nanoparticles. Results indicated that the superhydrophobic surface retained less residue compared to the uncoated surface after water cleaning, with dust easily removable by flipping the coated surface. These self-cleaning surfaces have various applications in the textile industry. Gao and al. [100] developed superhydrophobic surfaces utilizing a hierarchical structure of polydimethylsiloxane (PDMS) and silica particles on glass slides. Their findings indicated that 14 nm particles yield a higher contact angle than 7 nm particles, attributed to the regularity of their micro and nanostructures. In contrast, the 7 nm silica-PDMS particles exhibit more grooves and irregularities, reducing the air pockets that support water droplets. Najafian and al. [101] developed a $CuBi_2O_4/Bi_3ClO_4$ nanocomposite photocatalyst through an enhanced Pechini sol-gel process, utilizing a mixture of gelling agents and polybasic acids. This photocatalyst effectively removed the brown dye of 14-azoic acid, a water pollutant, when exposed to visible light.

Recently developed F-PE/SiO_2 foam demonstrates superhydrophobicity under high pressure, exhibiting a contact angle of 158 ±2 °and a sliding angle of 4 ±2 °[102]. It shows exceptional mechanical durability against scratches, peeling, flexural-torsion, and ultrasonication, maintaining its properties post-abrasion (Figure 10). The foam is suitable for applications in anti-wetting, self-cleaning, and anti-icing. Wang and al. [103] proposed a method to enhance strength using a robust inorganic adhesive combined with a self-similar repairable structure produced via nanoparticle spraying (see Figure 10). The adhesive's effectiveness is achieved through TEOS hydrolysis, resulting in stronger bonds. The structure can be remodeled after wear, demonstrating five times greater mechanical strength and persistent superamphiphobicity despite environmental exposure.

Wang and al. [104] created a coating using TiO_2, water-based polyurethane, and γ-aminopropyltriethoxysilane. This coating made cotton fabrics superhydrophobic, durable, frost-resistant, and waterproof for various uses. (see Figure 10).

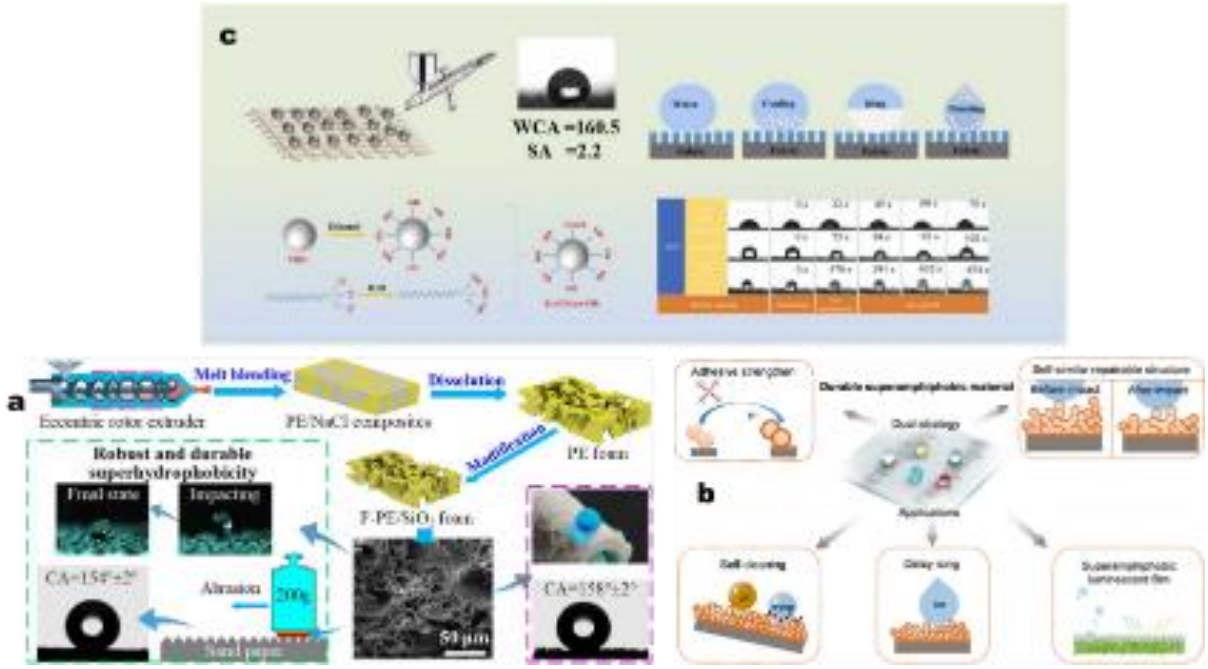

Figure 10. *Diagram illustrating a robust and durable superhydrophobic F-PE/SiO_2 foam with self-cleaning and anti-frosting behaviors [102]; (b) Durable superamphiphobic material obtained thru a dual strategy [103]; (c) Superhydrophobic, durable, and fluorine-free cotton fabrics [104].*

5.2. Anti-icing

Ice formation presents significant challenges, particularly in aviation, where it can accumulate on aircraft wings and fuselage from conditions like freezing rain and fog. This accumulation can result in weight increase and reduced lift, potentially causing a sudden loss of control. Additionally, ice ingestion into engines can lead to reduced thrust or complete power loss [105, 106]. Thus, the accumulation of ice on energy transmission systems, vehicles, or offshore platforms can cause considerable damage and potentially endanger people [107, 108].

The conventional approach to anti-icing is primarily based on a melting method that requires significant energy but is not entirely effective. Several biomimetic anti-icing mechanisms have been identified in recent years, including anti-icing [37] (Figure 11) (preventing droplets from adhering to the surface and directly removing them before they freeze), suppressing ice nucleation (delaying the crystallization of water droplets, which prolongs the freezing duration) and ice removal (reduc-

ing the adhesion force between the ice and the surface, allowing the ice to detach easily). Superhydrophobic coatings on a steel substrate were developed by Xi et al. [109] using HVOF thermal spraying, achieving a contact angle of 154.3 ±3 °and a sliding angle of 4.1 ±0.1 °. These coatings offer a significant 1206.4 seconds freezing delay in static conditions 8 times greater than the substrateand a reduced ice shear of 0.201 MPa at -15 ℃ for 1 hour, alongside effective frost weight reduction and ice repulsion.

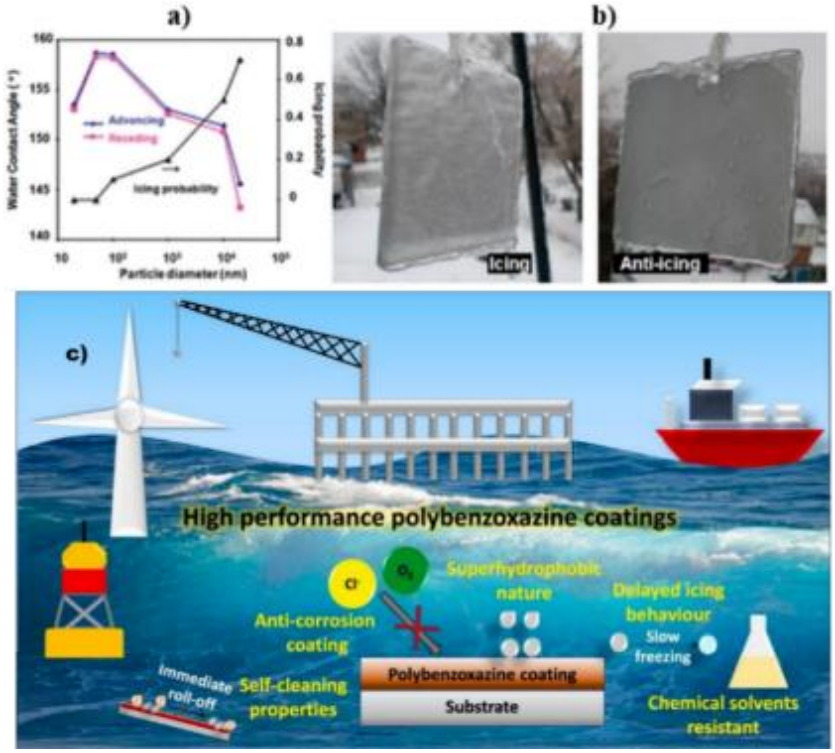

Figure 11. *Contact angles with water at the advancing and receding of particle-polymer composites as a function of particle size (a); (b) Testing of anti-icing properties in the case of natural "freezing rain" [110]; (c) Benzoxazines with a cardanol-phthalate core for superhydrophobic, corrosion-resistant, anti-icing, and self-cleaning coatings [111].*

Wang and al. [112] demonstrated that an increase in the height or a decrease in the diameter of a nanostructure led to a reduction in the defrosting temperature. Thus, to save energy during the defrosting process, the size of the surface nanostructures must be optimized. Such a structure also helps small water droplets converge into larger droplets and roll on the surface before they freeze, giving the surface an anti-icing property. An acrylic polymer-silica nanoparticle composite on a glass [110] or stainless steel substrate also exhibits anti-icing properties. Li and al. [113] presented a photothermal superhydrophobic coating developed with boron carbide microparticles and soot nanoparticles. This coating delays ice formation up to 5.77 times better than bare surfaces and facilitates rapid de-icing, while being resistant and stable under harsh conditions. For example, Nguyen and al. [114] showed a simple way to create a superhydrophobic surface to prevent icing using a custom device. They treated aluminum plates with wet etching and a low-energy compound, resulting in excellent hydrophobic properties. Slippery liquid-infused surfaces can also be made for anti-icing. Khammas and al. [115] used a flame and cold spraying method to produce polymer coatings impregnated with a silicone-based lubricant that exhibit potential SLIPS design performance. They argued that these SLIPS can be used as a solution in passive anti-icing due to their low adhesion to ice after several de-icing cycles.

Moreover, in order to address the issue related to aluminum, which is easily susceptible to corrosion, biofouling, and the deposition of foreign elements, thereby reducing its durability when it comes into contact with liquids. Radwan and al. [116] developed a superhydrophobic coating resistant to corrosion using carbon nanotubes and poly (vinylidene fluoride-co-hexafluoropropylene), achieving a contact angle of about 156 ± 2 °. Appasamy and al. [111] created a new bisphenol from cardanol and phthalic anhydride to make coating materials (see Figure 11). Two amines were used to produce benzoxazines. The findings showed great thermal stability, superhydrophobic features, and improved corrosion resistance in the coatings.

5.3. Oil/water Separation Membrane

Due to numerous industrial activities related to oil, minerals, and pharmaceuticals generating large quantities of wastewater

emulsions that pose a significant threat to ecosystems, the separation of oils, particularly oil/water, is increasingly being sought using materials with special wettability to water and oil [117]. Thus, numerous series of superhydrophobic and superoleophilic materials are reported and used for oil/water separation. For example, Dai and al. [118] designed superhydrophobic and superoleophilic alkali-oxidized copper meshes coated with octadecylphosphonic acid (ODPA), achieving a water contact angle of 158.9 ° and 0 ° for oil. The production involved oxidizing the copper mesh in an NaOH and $K_2S_2O_8$ solution, followed by ODPA coating (Figure 12). These meshes are effective for separating various oil/water mixtures, maintaining high efficiency after 20 uses. Additionally, they exhibit self-cleaning properties, making them promising for industrial water treatment and oil spill remediation.

Furthermore, Zhao and al. [119] developed superhydrophobic and superoleophilic polyethylene meshes using pressing, scratching, and puncturing. These meshes efficiently separate strong acids, bases, and saturated brine from oil and can be reused for at least 30 cycles. Their high flow rate enables quick oil/water separation, showing great industrial potential.

Other studies have shown the possibility of developing multifunctional superhydrophobic and superoleophilic surfaces with excellent self-cleaning capabilities, achieving a high oil/water separation efficiency of over 95% over 20 separation cycles by spraying stainless steel meshes [120] and with polyepoxy resin (PER) [121], achieving an excellent separation efficiency of 99.99% and a high flow rate of over 2000 L/(m^2h) under the effect of gravity.

Nanostructured glass microfiber membranes (GMF), enhanced through oxygen plasma treatment and a self-assembled monolayer coating, enable effective oil/water separation. Modifications by Woo et al. [122] created a nanostructured surface with excellent superhydrophobicity (see Figure 12). The optimized membrane achieved a high water intrusion pressure (< 62.7 kPa) and demonstrated impressive separation capabilities with high flux (< 4418 Lh^{-1} m^{-2}) and oil purity (> 99%). Additionally, it exhibited strong chemical stability under extreme acidic/alkaline and corrosive conditions. Ren and al. [123] developed a biomass aerogel called MH-TCP, designed for effective oil-water separation. This material features stable hydrophobic properties, mechanical strength, and self-healing capabilities. It achieved over 80% separation efficiency in tests and maintained its effectiveness through multiple cycles.

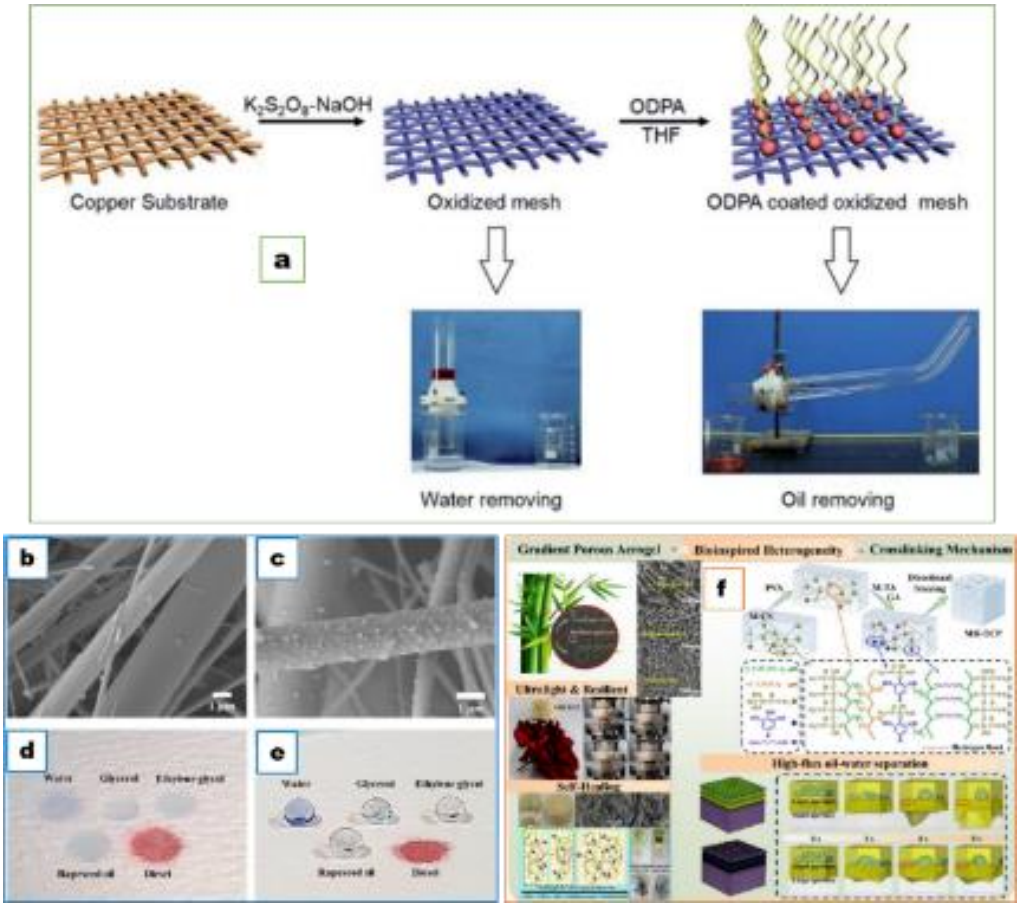

Figure 12. *Diagram illustrating the formation of an oil-water separation membrane: (a) ODPA coating on a copper mesh oxidized with alkali [118]; (b, c, d, e) SEM images of the pristine GMF membrane and the modified GMF membrane [122]; (f) Biomass-based heterogeneous aerogels with a porous gradient inspired by biology for high-throughput oil-water separation and self-healing [123].*

5.4. Water Collection System

Water collection through surfaces with strong water adhesion addresses the growing demand for clean water, driven by population growth, pollution, and climate change [124]. These surfaces capture water droplets, enabling recovery after tilting. The method relies on condensing atmospheric moisture, involving three stages: vapor condensation into droplets, growth of adhered droplets, and their subsequent falling. Effective water collection hinges on rapid condensation, growth, and removal of droplets [125-129].

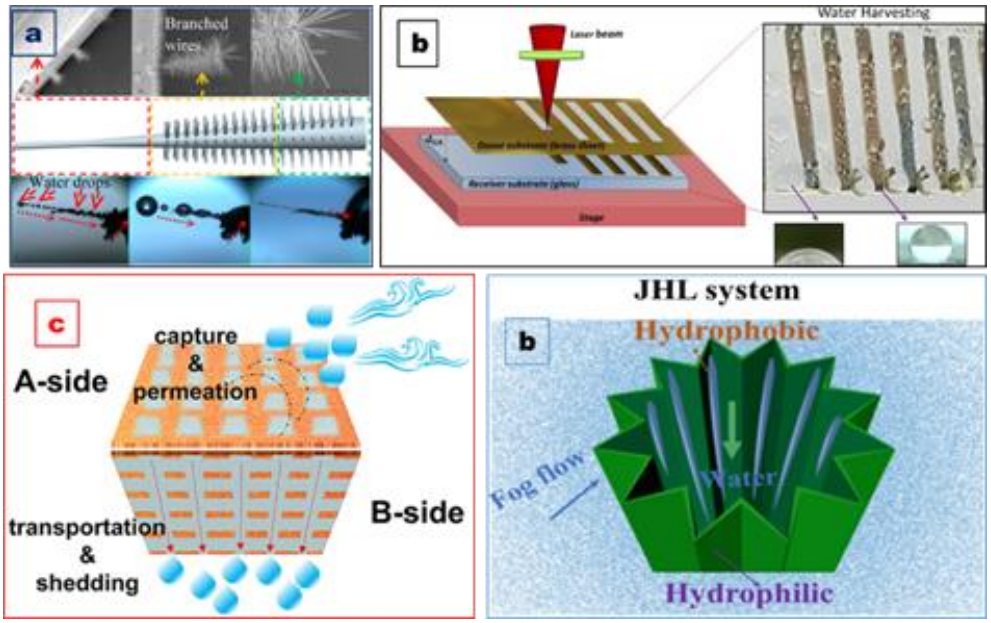

Figure 13. *Diagram illustrating the fabrication of a water collection system: (a) Large ZnO wire with small branches collects water [130]; (b) Superhydrophobic/hydrophilic hybrid patterns deposited on glass by the laser-induced direct transfer method [134]; (c) Janus surface with intertwined double structure and multi-biomimetic (Copyright © 2024 American Chemical Soiety) [135]; Janus membrane in origami form effective for fog collection (Copyright © 2025 American Chemical Society) [136].*

Studies show that artificial surfaces can mimic natural creatures' water collection abilities through two wettability states. For example, Heng and al. [130] imitated the unique structural characteristics of cactus spines as small one-dimensional structures to trap and transport water droplets (Figure 13). Another approach involves using wettability-modeled surfaces inspired by Namib Desert beetles, which possess efficient water collection capabilities in extremely dry conditions [131-133]. Furthermore, Hydrophobic materials with moderate hydrophilic groups improve droplet nucleation and removal better than natural materials [17]. They use restricted hydrophilic areas for fog condensation and achieve high water collection efficiency.

Recently, Bakhtiari and al. [134] created glass surfaces with different wettability to enhance water droplet recovery using a simple method (see Figure 13). They applied geometric patterns on glass with a laser technique and treated them with stearic acid to change their properties. The results indicated a 300% improvement in water recovery.

Gao and al. [135] created a two interwoven wetting Janus surface (DIWJS) that effectively collects fog (see Figure 13). Face A has superhydrophilic points, and face B has superhydrophilic stripes, which promotes the capture and evacuation of droplets. A smart farm model shows the many possible applications of DIWJS. Wang and al. [136] developed a fog collection system called Janus (JHL) that features treated surfaces for rapid water capture (see Figure 13). It has a 3D origami design and achieves high collection efficiency.

5.5. Other Applications

In addition to the applications already described above, unique wetting materials have also demonstrated significant applications in biomedical, maritime, and other fields. Their applications are about to revolutionize the development of antifouling and antibiofouling [137-139]. These prevent the undesirable adhesion of microorganisms, plants, algae, and animals on submerged surfaces on ship hulls and other marine structures, which play an important role in health, environmental, and maritime safety. Firouzjaei and al. [140] developed a nanocomposite membrane using graphene oxide and Ag-MOF for antifouling. Recently, the group of Peer and al. [141] fabricated nanofibrous membranes based on polyvinyl butyral containing various concentrations of monocaprine thru

electrospinning. The results showed very good antifouling activity in addition to their already reported antibacterial activities in the literature [142, 143].

6. Conclusion

This review article provided an overview of some methods used to create anti-wetting surfaces from conductive polymers, in the form of nanoparticles, nanocrystals, or the polymer itself, in order to develop anti-wetting coatings. The different techniques used to synthesize these anti-wetting surfaces based on conductive polymers have been schematically described in this article. Several characteristics such as self-cleaning, corrosion protection, membranes for separating oil and water, and anti-icing, obtained with anti-wetting coatings made from conductive polymer-based materials, have been highlighted. As the demand for electric vehicles rises, the demand for sensors with self-cleaning coatings has also increased over the years. Thanks to advancements in the fields of textiles and footwear, the demand for water-repellent coatings has gained significant importance. In the textile industry, anti-wetting coatings seem promising for saving water and energy used for cleaning, which reduces washing needs, and should be durable and resistant. In the face of the increasing demand for bioinspired anti-wetting surfaces, it is crucial to examine in more detail the advantages of conductive polymer-based materials and to participate in preserving the balance between technological progress and environmental protection.

Abbreviations

γ	Surface Energy
θ	Contact Angle
θa	Advance Angle
θr	Retraction Contact Angle
θγ	Young's Contact Angle
θw	Wenzel Contact Angle
θCB	Cassie-Baxter Contact Angle
γSV	Surface Tension at Solid-Vapor Interfaces
γSL	Surface Tension at Solid-Liquid Interfaces
γLV	Surface Tension at Liquid-Vapor Interfaces
H	Contact Angle Hysteresis
PDMS	PolyDiMéthylSiloxane
PVDF	PolyVinyliDeneFluoride
r	Roughness Factor
SAM	Self-Assembled Monolayer
SEM	Scanning Electron Microscopy
SiO_2	Silicon Dioxide
SLIPS	Slippery Liquid-Infused Porous Surfaces
TEOS	TetraEthyl OrthoSilicate
TiO_2	Titanium Dioxide

Author Contributions

Diawo Diallo: Conceptualization, Investigation, Visualization
Djibril Diouf: Supervision, Validation
Abdoulaye Drame: Supervision, Validation
Alioune Diouf: Supervision, Validation

Conflicts of Interest

The authors declare no conflicts of interest.

References

[1] Koch K, Bhushan B, Barthlott W. Multifunctional surface structures of plants: An inspiration for biomimetics. Progress in Materials Science 2009; 54: 137–78. https://doi.org/10.1016/j.pmatsci.2008.07.003

[2] Barthlott W. The purity of sacred lotus: superhydrophobic self-cleaning plant surfaces and the consequences revisited. Planta 2026; 263: 80. https://doi.org/10.1007/s00425-026-04937-9

[3] Cho WK, Choi IS. Fabrication of hairy polymeric films inspired by geckos: wetting and high adhesion properties. Advanced Functional Materials 2008; 18: 1089–96. https://doi.org/10.1002%2Fadfm.200701454

[4] Gao H, Wang X, Yao H, Gorb S, Arzt E. Mechanics of hierarchical adhesion structures of geckos. Mechanics of Materials 2005; 37: 275–85. https://doi.org/10.1016/j.mechmat.2004.03.008

[5] Cassie ABD, Baxter S. Wettability of porous surfaces. Transactions of the Faraday Society 1944; 40: 546–51. https://doi.org/10.1039/TF9444000546

[6] Fang W, Guo H-Y, Li B, Li Q, Feng X-Q. Revisiting the Critical Condition for the Cassie–Wenzel Transition on Micropillar-Structured Surfaces. Langmuir 2018; 34: 3838–44. https://doi.org/10.1021/acs.langmuir.8b00121

[7] Sethi SK, Manik G. Recent Progress in Super Hydrophobic/Hydrophilic Self-Cleaning Surfaces for Various Industrial Applications: A Review. Polymer-Plastics Technology and Engineering 2018; 57: 1932–52. https://doi.org/10.1080/03602559.2018.1447128

[8] Behera A. Self-Cleaning Materials. In: Behera A, editor. Advanced Materials: An Introduction to Modern Materials Science, Cham: Springer International Publishing; 2022, p. 359–94. https://doi.org/10.1007/978-3-030-80359-9_11

[9] Kosasih B, Novareza O, Tieu AK, Zhu H. Friction and anti-wear property of aqueous tri-block copolymer solutions in metal forming. International Journal of Surface Science and Engineering 2014; 8: 109–23. https://doi.org/10.1504/IJSURFSE.2014.060480

[10] Jiao Y, Zhang T, Ji J, Guo Y, Wang Z, Tao T, et al. Functional Microtextured Superhydrophobic Surface with Excellent Anti-Wear Resistance and Friction Reduction Properties. Langmuir 2022; 38: 13166–76. https://doi.org/10.1021/acs.langmuir.2c01959

[11] Shen L, Wang B, Wang J, Fu J, Picart C, Ji J. Asymmetric Free-Standing Film with Multifunctional Anti-Bacterial and Self-Cleaning Properties. ACS Appl Mater Interfaces 2012; 4: 4476–83. https://doi.org/10.1021/am301118f

[12] Ramos Chagas G, Mor án Cruz G, Giraudon-Colas G, Savina F, Meallet-Renault R, Amigoni S, et al. Anti-bacterial and fluorescent properties of hydrophobic electrodeposited non-fluorinated polypyrenes. Applied Surface Science 2018; 452: 352–63. https://doi.org/10.1016/j.apsusc.2018.04.268

[13] Zhou S, Wang F, Balachandran S, Li G, Zhang X, Wang R, et al. Facile fabrication of hybrid PA6-decorated TiO 2 fabrics with excellent photocatalytic, anti-bacterial, UV light-shielding, and super hydrophobic properties. RSC Adv 2017; 7: 52375–81. https://doi.org/10.1039/C7RA09613E

[14] Yu D, Tian J. Superhydrophobicity: Is it really better than hydrophobicity on anti-corrosion? Colloids and Surfaces A: Physicochemical and Engineering Aspects 2014; 445: 75–8. https://doi.org/10.1016/j.colsurfa.2014.01.016

[15] Zhang D, Yuan T, Wei G, Wang H, Gao L, Lin T. Preparation of self-healing hydrophobic coating on AA6061 alloy surface and its anti-corrosion property. Journal of Alloys and Compounds 2019; 774: 495–501. https://doi.org/10.1016/j.jallcom.2018.10.080

[16] Zhu H, Guo Z. Understanding the separations of oil/water mixtures from immiscible to emulsions on super-wettable surfaces. J Bionic Eng 2016; 13: 1–29. https://doi.org/10.1016/S1672-6529(14)60156-6

[17] Lyu P, Zhang X, Jiang X, Shang B, Liu X, Deng Z. One-Step Preparation of Hydrophobic Surfaces Containing Hydrophilic Groups for Efficient Water Harvesting. Langmuir 2021; 37: 9630–6. https://doi.org/10.1021/acs.langmuir.1c01756

[18] Gu J, Gu H, Cao J, Chen S, Li N, Xiong J. Robust hydrophobic polyurethane fibrous membranes with tunable porous structure for waterproof and breathable application. Applied Surface Science 2018; 439: 589–97. https://doi.org/10.1016/j.apsusc.2017.12.267

[19] Zhao J, Wang X, Xu Y, He P, Si Y, Liu L, et al. Multifunctional, Waterproof, and Breathable Nanofibrous Textiles Based on Fluorine-Free, All-Water-Based Coatings. ACS Appl Mater Interfaces 2020; 12: 15911–8. https://doi.org/10.1021/acsami.0c00846

[20] Bandyopadhyay S, Pallavi P, Anil AG, Patra A. Fabrication of porous organic polymers in the form of powder, soluble in organic solvents and nanoparticles: a unique platform for gas adsorption and efficient chemosensing. Polymer Chemistry 2015; 6: 3775–80. https://doi.org/10.1039/C5PY00235D

[21] Li Z, Li H, Xia H, Ding X, Luo X, Liu X, et al. Triarylboron-Linked Conjugated Microporous Polymers: Sensing and Removal of Fluoride Ions. Chemistry A European J 2015; 21: 17355–62. https://doi.org/10.1002/chem.201502241

[22] Shigrekar M, Amdoskar V. A review on recent progress and techniques used for fabricating superhydrophobic coatings derived from biobased materials. RSC Adv 2024; 14: 32668–99. https://doi.org/10.1039/D4RA04767B

[23] Bidan G. Composite materials containing electrically conductive polymers: a literature review. J Chim Phys 1989; 86: 45–60. https://doi.org/10.1051/jcp/1989860045

[24] Darmanin T, Godeau G, Guittard F. Superhydrophobic, superoleophobic and underwater superoleophobic conducting polymer films. Surface Innovations 2018; 6: 181–204. https://doi.org/10.1680/jsuin.18.00006

[25] Hu DL, Chan B, Bush JW. The hydrodynamics of water strider locomotion. Nature 2003; 424: 663–6. https://doi.org/10.1038/nature01793

[26] Bixler GD, Bhushan B. Fluid drag reduction and efficient self-cleaning with rice leaf and butterfly wing bioinspired surfaces. Nanoscale 2013; 5: 7685. https://doi.org/10.1039/c3nr01710a

[27] Barthwal S, Uniyal S, Barthwal S. Nature-Inspired Superhydrophobic Coating Materials: Drawing Inspiration from Nature for Enhanced Functionality. Micromachines 2024; 15: 391. https://doi.org/10.3390/mi15030391

[28] Barthlott W, Neinhuis C. Purity of the sacred lotus, or escape from contamination in biological surfaces. Planta 1997; 202: 1–8. https://doi.org/10.1007/s004250050096

[29] Feng L, Zhang Y, Xi J, Zhu Y, Wang N, Xia F, et al. Petal Effect: A Superhydrophobic State with High Adhesive Force. Langmuir 2008; 24: 4114–9. https://doi.org/10.1021/la703821h

[30] Wagner T, Neinhuis C, Barthlott W. Wettability and contaminability of insect wings as a function of their surface sculptures. Acta Zoologica 1996; 77: 213–25. https://doi.org/10.1111/j.1463-6395.1996.tb01265.x

[31] Oh J, Dana CE, Hong S, Roman JK, Jo KD, Hong JW, et al. Exploring the role of habitat on the wettability of cicada wings. ACS Applied Materials & Interfaces 2017; 9: 27173–84. https://doi.org/10.1021/acsami.7b07060

[32] Zheng Y, Gao X, Jiang L. Directional adhesion of superhydrophobic butterfly wings. Soft Matter 2007; 3: 178–82. https://doi.org/10.1039/B612667G

[33] Liu M, Wang S, Wei Z, Song Y, Jiang L. Bioinspired design of a superoleophobic and low adhesive water/solid interface. Advanced Materials 2009; 21: 665–9. https://doi.org/10.1002/adma.200801782

[34] Wen L, Weaver JC, Lauder GV. Biomimetic shark skin: design, fabrication and hydrodynamic function. Journal of Experimental Biology 2014; 217: 1656–66. https://doi.org/10.1242/jeb.097097

[35] Marmur A. Hydro- hygro- oleo- omni-phobic? Terminology of wettability classification. Soft Matter 2012; 8: 6867. https://doi.org/10.1039/c2sm25443c

[36] Zaman Khan M, Militky J, Petru M, Tomkov á B, Ali A, T ören E, et al. Recent advances in superhydrophobic surfaces for practical applications: A review. European Polymer Journal 2022; 178: 111481. https://doi.org/10.1016/j.eurpolymj.2022.111481

[37] Nguyen-Tri P, Tran HN, Plamondon CO, Tuduri L, Vo D-VN, Nanda S, et al. Recent progress in the preparation, properties and applications of superhydrophobic nano-based coatings and surfaces: A review. Progress in Organic Coatings 2019; 132: 235–56. https://doi.org/10.1016/j.porgcoat.2019.03.042

[38] Tuteja A, Choi W, Mabry JM, McKinley GH, Cohen RE. Robust omniphobic surfaces. Proc Natl Acad Sci USA 2008; 105: 18200–5. https://doi.org/10.1073/pnas.0804872105

[39] Surface chemistry: A close look at hydrophobicity. NPG Asia Mater 2011. https://doi.org/10.1038/asiamat.2011.25

[40] Ura DP, Stachewicz U. The Significance of Electrical Polarity in Electrospinning: A Nanoscale Approach for the Enhancement of the Polymer Fibers' Properties. Macro Materials & Eng 2022; 307: 2100843. https://doi.org/10.1002/mame.202100843

[41] Young T. III. An essay on the cohesion of fluids. Phil Trans R Soc 1805; 95: 65–87. https://doi.org/10.1098/rstl.1805.0005

[42] Vazirinasab E, Jafari R, Momen G. Application of superhydrophobic coatings as a corrosion barrier: A review. Surface and Coatings Technology 2018; 341: 40–56. https://doi.org/10.1016/j.surfcoat.2017.11.053

[43] Gao L, McCarthy TJ. Contact Angle Hysteresis Explained. Langmuir 2006; 22: 6234–7. https://doi.org/10.1021/la060254j

[44] Guittard F, Amigoni S, Darmanin T. Switchable and reversible wetting properties. Responsive Materials 2026; 4: e70028. https://doi.org/10.1002/rpm2.70028

[45] Koch K, Bhushan B, Barthlott W. Diversity of structure, morphology and wetting of plant surfaces. Soft Matter 2008; 4: 1943. https://doi.org/10.1039/b804854a

[46] Dettre RH, Johnson Jr RE. Contact angle hysteresis: II. Contact angle measurements on rough surfaces, ACS Publications; 1964. https://pubs.acs.org/doi/abs/10.1021/ba-1964-0043.ch008

[47] Ma M, Hill RM. Superhydrophobic surfaces. Current Opinion in Colloid & Interface Science 2006; 11: 193–202. https://doi.org/10.1016/j.cocis.2006.06.002

[48] Roach P, Shirtcliffe NJ, Newton MI. Progess in superhydrophobic surface development. Soft Matter 2008; 4: 224–40. https://doi.org/10.1039/B712575P

[49] Xu W, Ning T, Yang X, Lu S. Fabrication of superhydrophobic surfaces on zinc substrates. Applied Surface Science 2011; 257: 4801–6. https://doi.org/10.1016/j.apsusc.2010.12.059

[50] Celia E, Darmanin T, Taffin de Givenchy E, Amigoni S, Guittard F. Recent advances in designing superhydrophobic surfaces. Journal of Colloid and Interface Science 2013; 402: 1–18. https://doi.org/10.1016/j.jcis.2013.03.041

[51] Latthe S, Terashima C, Nakata K, Fujishima A. Superhydrophobic Surfaces Developed by Mimicking Hierarchical Surface Morphology of Lotus Leaf. Molecules 2014; 19: 4256–83. https://doi.org/10.3390/molecules19044256

[52] Latthe SS, Sudhagar P, Devadoss A, Kumar AM, Liu S, Terashima C, et al. A mechanically bendable superhydrophobic steel surface with self-cleaning and corrosion-resistant properties. Journal of Materials Chemistry A 2015; 3: 14263–71. https://doi.org/10.1039/C5TA02604K

[53] Zhang Y, Zhang Z, Yang J, Yue Y, Zhang H. Fabrication of superhydrophobic surface on stainless steel by two-step chemical etching. Chemical Physics Letters 2022; 797: 139567. https://doi.org/10.1016/j.cplett.2022.139567

[54] Liu H, Gao S-W, Cai J-S, He C-L, Mao J-J, Zhu T-X, et al. Recent Progress in Fabrication and Applications of Superhydrophobic Coating on Cellulose-Based Substrates. Materials 2016; 9: 124. https://doi.org/10.3390/ma9030124

[55] Wang Q, Yao X, Liu H, Quere D, Jiang L. Self-removal of condensed water on the legs of water striders. Proceedings of the National Academy of Sciences 2015; 112: 9247–52. https://doi.org/10.1073/pnas.1506874112

[56] Lee S-J, Kim C-W, Kim C-L. Development of mechanically robust superhydrophobic SUS 316 surfaces through chemical etching and fluorinated self-assembled monolayer. Phys Scr 2026; 101: 165909. https://doi.org/10.1088/1402-4896/ae5bd2

[57] Burdin L, Brulez A-C, Mazurczyk R, Leclercq J-L, Benayoun S. How the Structure and Wettability Properties of Morpho peleides Butterfly Wings Can Be a Source of Inspiration. Biomimetics 2025; 10: 89. https://doi.org/10.3390/biomimetics10020089

[58] Cheng J, Zhu Y, Zhan F, Wang L. Lotus leaf-inspired thermal insulation and anti-icing topography. RSC Adv 2024; 14: 18798–806. https://doi.org/10.1039/D4RA02843K

[59] Lee Y, Ju K-Y, Lee J-K. Stable biomimetic superhydrophobic surfaces fabricated by polymer replication method from hierarchically structured surfaces of Al templates. Langmuir 2010; 26: 14103–10. https://doi.org/10.1021/la102057p

[60] Peng C-W, Chang K-C, Weng C-J, Lai M-C, Hsu C-H, Hsu S-C, et al. Nano-casting technique to prepare polyaniline surface with biomimetic superhydrophobic structures for anticorrosion application. Electrochimica Acta 2013; 95: 192–9. https://doi.org/10.1016/j.electacta.2013.02.016

[61] Chen H, Li X, Li D. Superhydrophilic–superhydrophobic patterned surfaces: From simplified fabrication to emerging applications. Nanotechnology and Precision Engineering 2022; 5: 035002. https://doi.org/10.1063/10.0013222

[62] Zhang X, Wei C, Hao Y-J, Yan Z-W, Yan X, Chen Y, et al. Robust superhydrophobic PVDF membrane constructed by template-assisted strategy via thermally induced phase separation for rapid water-in-oil emulsions separation. Chemical Engineering Science 2023; 282: 119325. https://doi.org/10.1016/j.ces.2023.119325

[63] Dai S, Zhu Y, Gu Y, Du Z. Biomimetic fabrication and photoelectric properties of superhydrophobic ZnO nanostructures on flexible PDMS substrates replicated from rose petal. Appl Phys A 2019; 125: 138. https://doi.org/10.1007/s00339-019-2438-7

[64] Liu L, Kong G, Zhu Y, Che C. Superhydrophobic graphene aerogel beads for adsorption of oil and organic solvents via a convenient in situ sol-gel method. Colloid and Interface Science Communications 2021; 45: 100518. https://doi.org/10.1016/j.colcom.2021.100518

[65] Li J, Ding H, Zhang H, Guo C, Hong X, Sun L, et al. Superhydrophobic Methylated Silica Sol for Effective Oil–Water Separation. Materials 2020; 13: 842. https://doi.org/10.3390/ma13040842

[66] Ceratti DR, Louis B, Paquez X, Faustini M, Grosso D. A new dip coating method to obtain large-surface coatings with a minimum of solution. Advanced Materials 2015; 27: 4958–62. https://doi.org/10.1002/adma.201502518

[67] Gaulding EA, Diroll BT, Goodwin ED, Vrtis ZJ, Kagan CR, Murray CB. Deposition of wafer-scale single-component and binary nanocrystal superlattice thin films via dip-coating. Advanced Materials 2015; 27: 2846–51. https://doi.org/10.1002/adma.201405575

[68] Dey M, Doumenc F, Guerrier B. Numerical simulation of dip-coating in the evaporative regime. The European Physical Journal E 2016; 39: 1–9. https://doi.org/10.1140/epje/i2016-16019-4

[69] Tang X, Yan X. Dip-coating for fibrous materials: mechanism, methods and applications. J Sol-Gel Sci Technol 2017; 81: 378–404. https://doi.org/10.1007/s10971-016-4197-7

[70] Lu Y, Ganguli R, Drewien CA, Anderson MT, Brinker CJ, Gong W, et al. Continuous formation of supported cubic and hexagonal mesoporous films by sol–gel dip-coating. Nature 1997; 389: 364–8. https://doi.org/10.1038/38699

[71] Almeida RM, Gonçalves MC, Portal S. Sol–gel photonic bandgap materials and structures. Journal of Non-Crystalline Solids 2004; 345: 562–9. https://doi.org/10.1016/j.jnoncrysol.2004.08.085

[72] Yeom C, Kim Y. Purification of oily seawater/wastewater using superhydrophobic nano-silica coated mesh and sponge. Journal of Industrial and Engineering Chemistry 2016; 40: 47–53. https://doi.org/10.1016/j.jiec.2016.06.005

[73] Martusciello M, Hervieu C, Di Fonzo D, Lanfranchi A, Lova P, Comoretto D. Dip-Coating Fabrication of All-Polymer Multilayer Photonic Crystals through 3D Printer Conversion. ACS Appl Polym Mater 2025; 7: 4779–86. https://doi.org/10.1021/acsapm.4c04077

[74] Rauh F, Bienek O, Sharp ID, Stutzmann M. Conversion of a 3D printer for versatile automation of dip coating processes. Review of Scientific Instruments 2023; 94: 083901. https://doi.org/10.1063/5.0128116

[75] Mohilner DM, Adams RN, Argersinger WJ. Investigation of the Kinetics and Mechanism of the Anodic Oxidation of Aniline in Aqueous Sulfuric Acid Solution at a Platinum Electrode. J Am Chem Soc 1962; 84: 3618–22. https://doi.org/10.1021/ja00878a003

[76] Sagisaka M, Darmanin T, Guittard F, Eastoe J. New fluorine-free low surface energy surfactants and surfaces. Journal of Colloid and Interface Science 2025; 690: 137229. https://doi.org/10.1016/j.jcis.2025.03.018

[77] Sabouraud G, Sadki S, Brodie N. The mechanisms of pyrrole electropolymerization. Chem Soc Rev 2000; 29: 283–93. https://doi.org/10.1039/a807124a

[78] Pringle JM, Efthimiadis J, Howlett PC, Efthimiadis J, MacFarlane DR, Chaplin AB, et al. Electrochemical synthesis of polypyrrole in ionic liquids. Polymer 2004; 45: 1447–53. https://doi.org/10.1016/j.polymer.2004.01.006

[79] Nobrega MM, Martins VL, Torresi RM, Temperini MLA. One-Step Synthesis, Characterization, and Properties of Emeraldine Salt Nanofibers Containing Gold Nanoparticles. J Phys Chem C 2014; 118: 4267–74. https://doi.org/10.1021/jp4120755

[80] Ding C, Qian X, Yu G, An X. Dopant effect and characterization of polypyrrole-cellulose composites prepared by in situ polymerization process. Cellulose 2010; 17: 1067–77. https://doi.org/10.1007/s10570-010-9442-6

[81] Carquigny S, Segut O, Lakard B, Lallemand F, Fievet P. Effect of electrolyte solvent on the morphology of polypyrrole films: Application to the use of polypyrrole in pH sensors. Synthetic Metals 2008; 158: 453–61. https://doi.org/10.1016/j.synthmet.2008.03.010

[82] Osagawara M, Funahashi K, Demura T, Hagiwara T, Iwata K. Enhancement of electrical conductivity of polypyrrole by stretching. Synthetic Metals 1986; 14: 61–9. https://doi.org/10.1016/0379-6779(86)90127-X

[83] Iacovetta D, Tam J, Erb U. Synthesis, structure, and properties of superhydrophobic nickel–PTFE nanocomposite coatings made by electrodeposition. Surface and Coatings Technology 2015; 279: 134–41. https://doi.org/10.1016/j.surfcoat.2015.08.022

[84] Darmanin T, Klimareva EL, Schewtschenko I, Guittard F, Perepichka IF. Exceptionally Strong Effect of Small Structural Variations in Functionalized 3,4-Phenylenedioxythiophenes on the Surface Nanostructure and Parahydrophobic Properties of Their Electropolymerized Films. Macromolecules 2019; 52: 8088–102. https://doi.org/10.1021/acs.macromol.9b00778

[85] Diallo D, Drame A, Diouf A, Sene A, Guittard F, Darmanin T. Directional growth of nanotubes on micelles by soft-template electropolymerization with varying hydrophobicity and strong water adhesion. New J Chem 2023; 47: 17685–92. https://doi.org/10.1039/D3NJ01186K

[86] Diallo D, Diouf A, Drame A, Sene A, Guittard F, Darmanin T. Bioinspired Nanostructures by Soft-Template Electropolymerization from Di-Substituted Triphenylamine. ChemistrySelect 2024; 9: e202402736. https://doi.org/10.1002/slct.202402736

[87] Darmanin T, Guittard F. A one-step electrodeposition of homogeneous and vertically aligned nanotubes with parahydrophobic properties (high water adhesion). J Mater Chem A 2016; 4: 3197–203. https://doi.org/10.1039/C5TA09253A

[88] Szczepanski CR, M'Jid I, Darmanin T, Godeau G, Guittard F. A template-free approach to nanotube-decorated polymer surfaces using 3, 4-phenylenedioxythiophene (PhEDOT) monomers. J Mater Chem A 2016; 4: 17308–23. https://doi.org/10.1039/C6TA07639D

[89] Fradin C, Orange F, Amigoni S, Szczepanski CR, Guittard F, Darmanin T. Micellar formation by soft template electropolymerization in organic solvents. Journal of Colloid and Interface Science 2021; 590: 260–7. https://doi.org/10.1016/j.jcis.2021.01.038

[90] Sow S, Drame A, Thiam E hadji Y, Orange F, Sene A, Dieng SY, et al. Nanotubular structures via templateless electropolymerization using thieno [3] thiophene monomers with various substituents and polar linkers. Progress in Organic Coatings 2020; 138: 105382. https://doi.org/10.1016/j.porgcoat.2019.105382

[91] Sane O, Diouf A, Pan M, Cruz GM, Savina F, Meallet-Renault R, et al. Nanotubular structures through templateless electropolymerization using thieno [3] thiophene derivatives with different substituents and water content. Electrochimica Acta 2019; 320: 134594. https://doi.org/10.1016/j.electacta.2019.134594

[92] Gbilimou A, Darmanin T, Godeau G, Guittard F. A templateless electropolymerization Approach to nanorings using substituted 3, 4-naphthalenedioxythiophene (NaPhDOT) monomers. ChemNanoMat 2018; 4: 140–7. https://doi.org/10.1002/cnma.201700269

[93] Chagas GR, Darmanin T, Godeau G, Guittard F. Nanocups and hollow microspheres formed by a one-step and templateless electropolymerization of thieno [3] thiophene derivatives as a function of the substituent. Electrochimica Acta 2018; 269: 462–78. https://doi.org/10.1016/j.electacta.2018.03.036

[94] Kumar Sharma G, Rachel James N. Electrospinning: The Technique and Applications. In: Khan M, Jerold Samuel Chelladurai S, editors. Recent Developments in Nanofibers Research, IntechOpen; 2023. https://doi.org/10.5772/intechopen.105804

[95] Venmathi Maran BA, Jeyachandran S, Kimura M. A Review on the Electrospinning of Polymer Nanofibers and Its Biomedical Applications. J Compos Sci 2024; 8: 32. https://doi.org/10.3390/jcs8010032

[96] Zeng Q, Zhou H, Huang J, Guo Z. Review on the recent development of durable superhydrophobic materials for practical applications. Nanoscale 2021; 13: 11734–64. https://doi.org/10.1039/D1NR01936H

[97] Bhushan B, Jung YC. Natural and biomimetic artificial surfaces for superhydrophobicity, self-cleaning, low adhesion, and drag reduction. Progress in Materials Science 2011; 56: 1–108. https://doi.org/10.1016/j.pmatsci.2010.04.003

[98] Xiu Y, Hess DW, Wong CP. A novel method to prepare superhydrophobic, self-cleaning and transparent coatings for biomedical applications. 2007 Proceedings 57th Electronic Components and Technology Conference, IEEE; 2007, p. 1218–23. https://doi.org/10.1109/ECTC.2007.373949

[99] Nimittrakoolchai O-U, Supothina S. Deposition of organic-based superhydrophobic films for anti-adhesion and self-cleaning applications. Journal of the European Ceramic Society 2008; 28: 947–52. https://doi.org/10.1016/j.jeurceramsoc.2007.09.025

[100] Gao N, Yan YY, Chen XY, Mee DJ. Superhydrophobic surfaces with hierarchical structure. Materials Letters 2011; 65: 2902–5. https://doi.org/10.1016/j.matlet.2011.06.088

[101] Najafian H, Manteghi F, Beshkar F, Salavati-Niasari M. Fabrication of nanocomposite photocatalyst $CuBi_2O_4/Bi_3ClO_4$ for removal of acid brown 14 as water pollutant under visible light irradiation. Journal of Hazardous Materials 2019; 361: 210–20. https://doi.org/10.1016/j.jhazmat.2018.08.092

[102] Wu T, Xu W, Guo K, Xie H, Qu J. Efficient fabrication of lightweight polyethylene foam with robust and durable superhydrophobicity for self-cleaning and anti-icing applications. Chemical Engineering Journal 2021; 407: 127100. https://doi.org/10.1016/j.cej.2020.127100

[103] Wang Y, Mao Y, Bi H, Chai Y, Jin Q, Li H, et al. Durable superamphiphobic material via a dual strengthen strategy for anti-icing and luminescent material self-cleaning. Applied Materials Today 2025; 45: 102817. https://doi.org/10.1016/j.apmt.2025.102817

[104] Wang X, Xue X, Li Y, Yan F, Liu H. A facile fabrication of durable, fluorine-free superhydrophobic cotton fabrics with integrated self-cleaning and anti-icing properties. Colloids and Surfaces A: Physicochemical and Engineering Aspects 2026; 733: 139267. https://doi.org/10.1016/j.colsurfa.2025.139267

[105] Sujata M, Madan M, Raghavendra K, Jagannathan N, Bhaumik SK. Unraveling the cause of an aircraft accident. Engineering Failure Analysis 2019; 97: 740–58. https://doi.org/10.1016/j.engfailanal.2019.01.065

[106] Cao Y, Tan W, Wu Z. Aircraft icing: An ongoing threat to aviation safety. Aerospace Science and Technology 2018; 75: 353–85. https://doi.org/10.1016/j.ast.2017.12.028

[107] Veerakumar R, Gao L, Liu Y, Hu H. Dynamic ice accretion process and its effects on the aerodynamic drag characteristics of a power transmission cable model. Cold Regions Science and Technology 2020; 169: 102908. https://doi.org/10.1016/j.coldregions.2019.102908

[108] Borrebæk P-OA, Jelle BP, Zhang Z. Avoiding snow and ice accretion on building integrated photovoltaics–Challenges, strategies, and opportunities. Solar Energy Materials and Solar Cells 2020; 206: 110306. https://doi.org/10.1016/j.solmat.2019.110306

[109] Xi N, Liu Y, Zhang X, Liu N, Fu H, Hang Z, et al. Steady anti-icing coatings on weathering steel fabricated by HVOF spraying. Applied Surface Science 2018; 444: 757–62. https://doi.org/10.1016/j.apsusc.2018.03.075

[110] Cao L, Jones AK, Sikka VK, Wu J, Gao D. Anti-icing superhydrophobic coatings. Langmuir 2009; 25: 12444–8. https://doi.org/10.1021/la902882b

[111] Appasamy S, Srinivasan H, Mydeen K M, Kumaravel A, Krishnan A, Muthukaruppan A. Cardanol-phthalein cored benzoxazines for superhydrophobic, corrosion resistant, anti-icing and self-cleaning coatings. European Polymer Journal 2026; 253: 114768. https://doi.org/10.1016/j.eurpolymj.2026.114768

[112] Wang F, Liang C, Yang W, Zhang X. Effects of frost thickness on dynamic defrosting on vertical hydrophobic and superhydrophobic fin surfaces. Energy and Buildings 2020; 223: 110134. https://doi.org/10.1016/j.enbuild.2020.110134

[113] Li Q, Pan J, Wang H, Chen T, Lu X. Scalable Fluorine-Free Superhydrophobic photo-thermal Coating Based on Boron Carbide and Candle Soot for Anti-Icing and photo-thermal De-Icing. Nanoscale 2026; 18: 11992-12008. https://doi.org/10.1039/D6NR01482H

[114] Nguyen V-H, Nguyen BD, Pham HT, Lam SS, Vo D-VN, Shokouhimehr M, et al. Anti-icing performance on aluminum surfaces and proposed model for freezing time calculation. Scientific Reports 2021; 11: 3641. https://doi.org/10.1038/s41598-021-88230-7

[115] Khammas R, Koivuluoto H. Durable Icephobic Slippery Liquid-Infused Porous Surfaces (SLIPS) Using Flame-and Cold-Spraying. Sustainability 2022; 14: 8422. https://doi.org/10.3390/su14148422

[116] Radwan AB, Ibrahim MA, Ismail EH, El Basiony NasserM, El-Hout SI, Zughaier SM, et al. Anticorrosion Properties of Robust and UV-Durable Poly (vinylidene fluoride-co-hexafluoropropylene)/Carbon Nanotubes Superhydrophobic Coating. Ind Eng Chem Res 2024; 63: 1380–95. https://doi.org/10.1021/acs.iecr.3c03280

[117] Guo X-Y, Zhao L, Li H-N, Yang H-C, Wu J, Liang H-Q, et al. Janus channel of membranes enables concurrent oil and water recovery from emulsions. Science 2024; 386: 654–9. https://doi.org/10.1126/science.adq6329

[118] Dai C, Liu N, Cao Y, Chen Y, Lu F, Feng L. Fast formation of superhydrophobic octadecylphosphonic acid (ODPA) coating for self-cleaning and oil/water separation. Soft Matter 2014; 10: 8116–21. https://doi.org/10.1039/x0xx00000x

[119] Zhao T, Zhang D, Yu C, Jiang L. Facile Fabrication of a Polyethylene Mesh for Oil/Water Separation in a Complex Environment. ACS Appl Mater Interfaces 2016; 8: 24186–91. https://doi.org/10.1021/acsami.6b07432

[120] Zhang Z, Wang H, Liang Y, Li X, Ren L, Cui Z, et al. One-step fabrication of robust superhydrophobic and superoleophilic surfaces with self-cleaning and oil/water separation function. Scientific Reports 2018; 8: 3869. https://doi.org/10.1038/s41598-018-22241-9

[121] Tian F, Yang Y, Wang X-L, An W-L, Zhao X, Xu S, et al. From waste epoxy resins to efficient oil/water separation materials *via* a microwave assisted pore-forming strategy. Mater Horiz 2019; 6: 1733–9. https://doi.org/10.1039/C9MH00541B

[122] Woo S, Park HR, Park J, Yi J, Hwang W. Robust and continuous oil/water separation with superhydrophobic glass microfiber membrane by vertical polymerization under harsh conditions. Scientific Reports 2020; 10: 21413. https://doi.org/10.1038/s41598-020-78271-9

[123] Ren J, Wang Z, Wu J, Xiao J, Chu Z, Wang Y. Bioinspired heterogeneous gradient-porous biomass aerogels for high-flux oil–water separation and self-healing. Separation and Purification Technology 2026; 397: 138121. https://doi.org/10.1016/j.seppur.2026.138121

[124] Mekonnen MM, Hoekstra AY. Four billion people facing severe water scarcity. Science Advances 2016; 2: e1500323. https://doi.org/10.1126/sciadv.1500323

[125] Kim H, Yang S, Rao SR, Narayanan S, Kapustin EA, Furukawa H, et al. Water harvesting from air with metal-organic frameworks powered by natural sunlight. Science 2017; 356: 430–4. https://doi.org/10.1126/science.aam8743

[126] Kim H, Rao SR, Kapustin EA, Zhao L, Yang S, Yaghi OM, et al. Adsorption-based atmospheric water harvesting device for arid climates. Nature Communications 2018; 9: 1191. https://doi.org/10.1038/s41467-018-03162-7

[127] Dai X, Sun N, Nielsen SO, Stogin BB, Wang J, Yang S, et al. Hydrophilic directional slippery rough surfaces for water harvesting. Science Advances 2018; 4: eaaq0919. https://doi.org/10.1126/sciadv.aaq0919

[128] Zhang S, Huang J, Chen Z, Lai Y. Bioinspired special wettability surfaces: from fundamental research to water harvesting applications. Small 2017; 13: 1602992. https://doi.org/10.1002/smll.201602992

[129] Tian Y, Zhu P, Tang X, Zhou C, Wang J, Kong T, et al. Large-scale water collection of bioinspired cavity-microfibers. Nature Communications 2017; 8: 1080. https://doi.org/10.1038/s41467-017-01157-4

[130] Heng X, Xiang M, Lu Z, Luo C. Branched ZnO wire structures for water collection inspired by cacti. ACS Applied Materials & Interfaces 2014; 6: 8032–41. https://doi.org/10.1021/am4053267

[131] Bai H, Wang L, Ju J, Sun R, Zheng Y, Jiang L. Efficient water collection on integrative bioinspired surfaces with star-shaped wettability patterns. Advanced Materials 2014; 26: 5025–30. https://doi.org/10.1002/adma.201400262

[132] Song Y, Liu Y, Jiang H, Li S, Kaya C, Stegmaier T, et al. Temperature-tunable wettability on a bioinspired structured graphene surface for fog collection and unidirectional transport. Nanoscale 2018; 10: 3813–22. https://doi.org/10.1039/C7NR07728A

[133] Wang M, Liu Q, Zhang H, Wang C, Wang L, Xiang B, et al. Laser direct writing of tree-shaped hierarchical cones on a superhydrophobic film for high-efficiency water collection. ACS Applied Materials & Interfaces 2017; 9: 29248–54. https://doi.org/10.1021/acsami.7b08116

[134] Bakhtiari N, Azizian S, Jaleh B. Hybrid superhydrophobic/hydrophilic patterns deposited on glass by laser-induced forward transfer method for efficient water harvesting. Journal of Colloid and Interface Science 2022; 625: 383–96. https://doi.org/10.1016/j.jcis.2022.06.039

[135] Gao H, Zhao H, Chang S, Meng Z, Han Z, Liu Y. Multi-biomimetic Double Interlaced Wetting Janus Surface for Efficient Fog Collection. Nano Lett 2024; 24: 7774–82. https://doi.org/10.1021/acs.nanolett.4c01918

[136] Wang Q, Zhang Y, Tian G, Guo Z. An Efficient Fog Collection Origami Janus Membrane for Rapid Directional Water Transport and Omnidirectional Fog Harvesting. ACS Appl Mater Interfaces 2025; 17: 42474–85. https://doi.org/10.1021/acsami.5c10459

[137] Soriano-Jerez Y, Gallardo-Rodríguez JJ, López-Rosales L, García-Camacho F, Bressy C, Molina-Grima E, et al. Preventing biofouling in microalgal photobioreactors. Bioresource Technology 2024; 407: 131125. https://doi.org/10.1016/j.biortech.2024.131125

[138] Vinagre PA, Simas T, Cruz E, Pinori E, Svenson J. Marine Biofouling: A European Database for the Marine Renewable Energy Sector. JMSE 2020; 8: 495. https://doi.org/10.3390/jmse8070495

[139] Scardino A, De Nys R, Ison O, O'Connor W, Steinberg P. Microtopography and antifouling properties of the shell surface of the bivalve molluscs Mytilus galloprovincialis and Pinctada imbricata. Biofouling 2003; 19: 221–30. https://doi.org/10.1080/0892701021000057882

[140] Firouzjaei MD, Shamsabadi AA, Aktij SA, Seyedpour SF, Sharifian Gh. M, Rahimpour A, et al. Exploiting Synergetic Effects of Graphene Oxide and a Silver-Based Metal–Organic Framework To Enhance Antifouling and Anti-Biofouling Properties of Thin-Film Nanocomposite Membranes. ACS Appl Mater Interfaces 2018; 10: 42967–78. https://doi.org/10.1021/acsami.8b12714

[141] Peer P, Sedlaříková J, Janalíková M, Kučerová L, Pleva P. Novel Polyvinyl Butyral/Monoacylglycerol Nanofibrous Membrane with Antifouling Activity. Materials 2020; 13: 3662. https://doi.org/10.3390/ma13173662

[142] Ding Q, Li W, Mei L, Luo S, Tao J, Shi C, et al. Tailoring Advanced Metal-Based Nanomedicines for Adaptable Nanodynamic Disease Therapies and Theranostics. Advanced Materials 2026; 38: e13609. https://doi.org/10.1002/adma.202513609

[143] Efunnuga A, Efunnuga A, Onivefu AP, Ifijen IH, Maliki M, Omorogbe SO, et al. Nanomedicine Advancements: Vanadium Oxide Nanoparticles as a Game-Changer in Antimicrobial and Anticancer Therapies. BioNanoSci 2024; 14: 3715–56. https://doi.org/10.1007/s12668-024-01566-y